Mine Water and the Environment (2022) 41:437–457
https://doi.org/10.1007/s10230-022-00859-6

TECHNICAL ARTICLE

Mercury Partitioning and Behavior in Streams and Source Areas Affected by the Novo-Ursk Gold Sulfide Tailings (West Siberia, Russia)

I. N. Myagkaya[1] · M. A. Gustaytis[1] · B. Yu. Saryg-ool[1] · E. V. Lazareva[1]

Received: 25 March 2021 / Accepted: 1 March 2022 / Published online: 1 April 2022

Abstract

We studied the behavior of mercury in acid mine drainage (AMD) and in portions of the Ur River affected and non-affected by AMD near the Ursk sulfide tailings (Siberia) before (2007–2009) and after (2011–2019) the beginning of tailings reprocessing operations. Mercury occurs in water as dissolved plus colloidal (Hg_{dc}) and colloidal (Hg_C) species or is adsorbed on suspended particles (Hg_{susp}). The mercury species were classified as either reactive (Hg_R) or non-reactive (Hg_{NR}), depending on their capacity to reduce to Hg^0 by reacting with $SnCl_2$. The composition and pH of the AMD and river waters change downstream of the AMD input. Mercury concentrations ranged from 1.8 to 89 µg/L (for the entire monitoring period) and increased with AMD pH. High-pH conditions are unfavorable for the precipitation of jarosite, which can adsorb Hg from water, and thus mercury remains mobile. Hg_{NR} is more abundant than Hg_R in the river and in AMD particulates. Non-reactive mercury in the river water is associated with CH_3Hg^+, which correlates with total organic carbon (TOC), while Hg in the AMD samples is bound to $HgS_{(s)}$, m-$HgS_{(s)}$, $HgSe_{(s)}$, and Hg-jarosite. Hg_R species are associated with particulates in all water bodies as $Hg^0_{(liq)}$, $Hg(OH)_{2(aq)}$, $HgCl_{2(aq)}$, and Hg^{2+} adsorbed by OH groups on the surfaces of mineral grains. Judging by the TOC concentration and the pH and Eh of river water, which local people use for fishing, Hg is prone to methylation upstream and downstream of the AMD input. The Hg enrichment of local surface waters is due to both a naturally elevated background in a Hg-rich province and to the mining and processing operations.

Keywords Acid mine drainage · Natural surface waters · Mercury species · Pollution · Long-term monitoring

Introduction

Environmental problems associated with acid mine drainage (AMD), especially the behavior of metals and potentially toxic elements (As, Hg, etc.), have attracted much research interest (Al et al. 2006; Boulet and Larocque 1998; Dutta et al. 2020; Gustaytis et al. 2010, 2013; Lazareva et al. 2002; Lusilao-Makiese et al. 2013). However, less attention has focused on the speciation of elements (Bavec et al. 2014; Kim et al. 2004) as bioavailability and toxicity proxies (Galán et al. 2003; Najamuddin et al. 2016; Sundaray et al. 2011), which are more informative than total concentrations.

High-sulfide tailings contain up to 0.7% mercury (Gustaytis et al. 2016), a very dangerous neurotoxin (Gustaytis et al. 2010, 2013, 2018, 2021; Gutiérrez-Mosquera et al. 2021; Qiu et al. 2013; Willis et al. 2019). Mercury occurs as diverse chemical species that experience especially active transformations in aqueous systems such as rivers, natural and manmade lakes, and wetlands (Bonzongo et al. 2006; La Colla et al. 2019).

Mercury has three main oxidation states: Hg^0, Hg^+, and Hg^{2+}; the latter is mainly bound to suspended particles or to dissolved organic matter (Ravichandran 2004) and is more abundant than Hg^+ in natural systems (Beckers and Rinklebe 2017). Water systems can contain Hg as inorganic or organic complexes (fulvic, etc.), Hg-organic compounds like mono- or dimethyls, or other substances with covalent Hg–C bonds (Laperdina 2000). Mercury can form complexes with fulvic or humic acids, which are, respectively, soluble or insoluble in water (Dobrovolsky 2004), and Hg complexed with humic and fulvic acids can be adsorbed on suspended particles (Ullrich et al. 2007). By reacting with methyl groups in fulvic and humic acids (Ullrich et al. 2001; Ravichandran

✉ I. N. Myagkaya
i_myagkaya@igm.nsc.ru

[1] V.S. Sobolev Institute of Geology and Mineralogy Siberian Branch, Russian Academy of Sciences, 3, Koptyug Ave, Novosibirsk 630090, Russia

2004), inorganic mercury species may convert to extremely toxic methylated forms (methylmercury).

Mercury interacts with solid phases by the mechanisms of ion exchange, complexation (with humic acids), or adsorption onto clay or other minerals. Furthermore, clay particles, iron and manganese hydroxides, metal humates, and seston (biotic and abiotic suspended particulates) can form colloids that adsorb mercury electrostatically (Ullrich et al. 2007).

Methylmercury is unstable under anaerobic conditions, such as in bottom sediment, and can convert to other organic compounds in the presence of H_2S (Baldi et al. 1995). Importantly, complexation of organic and inorganic Hg compounds with low-molecular-weight dissolved organic matter and thiols (thiovanic and thiopropion acids, cistein, and glutathion) can be mediated by bacteria (Jaliehvand et al. 2006; Kõszegi-Szalai and Paál 1999; Leung et al. 2007). Furthermore, Hg in sulfidic waters produces inorganic sulfides ($HgS_{(s)}$) and polysulfides, e.g. mononuclear complexes ($Hg(SH)_{2(aq)}$), or mixtures of mercury chlorides and sulfides ($HgClSH_{(aq)}$) (Paquette and Helz 1997).

Both CH_3Hg (II) and Hg (II) in soil and dissolved organic matter can bind with sulfur reduced by microorganisms (Hesterberg et al. 2001; Qian et al. 2002; Xia et al. 1999). Sulfate ions maintain Hg methylation in the presence of sulfate-reducing bacteria in bottom sediments (Gilmour et al. 1992) and peat soils (Branfierun et al. 2001). In this respect, the concentrations of natural organic matter and sulfur in soils or bottom sediments affect the mobility and stability of Hg.

Mercury associated with particulate matter in natural waters can be reactive (Hg_R) or non-reactive (Hg_{NR}). The classification for particulate matter reactivity is based on analytical treatment (Lindqvist and Rodhe 1985), whereby reactive Hg compounds are reduced to Hg^0 by $SnCl_2$ in acidic solution, while non-reactive Hg compounds are reduced to Hg^0 by $NaBH_4$ in alkaline solution. The reactive species and compounds include Hg^{2+}, HgX_2, HgX_3^-, and HgX_4^{2-} ($X = Cl^-$, OH^-, Br^-), HgC_2O_4 (Hg(II) oxalate), and Hg^{2+} complexed with organic acids, while the non-reactive compounds are $Hg(CN)_2$, HgS, Hg(II) bound with sulfur in humic compounds, CH_3Hg^+, CH_3HgCl, CH_3HgOH, and Hg bound with other organic substances. Non-reactive compounds can be transformed into reactive by concentrated HNO_3 (Lindqvist and Rodhe 1985). The sum of Hg^{2+} and Hg^0 is sometimes called inorganic mercury (Ferrari et al. 2000), which is determined as reactive mercury based on Hg^{2+} reduction to Hg^0 with $SnCl_2/HNO_3$ solution. However, it appears not quite correct to consider Hg_R and Hg_{NR} as purely inorganic mercury, because Hg-organic compounds and complexes (including those with Hg^{2+}) are present in both groups. The Hg-organic species are defined as those where Hg has covalent bonds with at least one carbon atom (World Health Organization 1990). In the study of Umezaki and Iwamoto (1971), inorganic and organic mercury were determined simultaneously. The procedure began with reducing inorganic mercury compounds by Sn(II) in 2 N sulfuric acid solution containing chloride ion; then both inorganic and organic mercury compounds were reduced by Sn(II) in 1 N sodium hydroxide solution containing traces of cupric ion; finally, the concentration of organic mercury was calculated from absorbance difference. Meanwhile, knowing total concentrations of mercury is less important for understanding the behavior of Hg in supergene environments than its speciation, because Hg species differ in environmental mobility.

The accumulation and speciation of mercury in water and sediments are controlled by such essential environmental parameters as pH, Eh, and concentrations of organic carbon and sulfur (Skyllberg et al. 2003). Correspondingly, the behavior of mercury can be studied by monitoring seasonal and long-term variations of these general parameters (Liu et al. 2017; Xu et al. 2019).

The aim of this study was to examine the long-term behavior of Hg and its dissolved, colloidal, and suspended species in the AMD – Ur River system to assess the impact of geochemical processes and long-term industrial activity on mercury pollution of natural river ecosystems. We report the results of long-term AMD monitoring in the Ursk tailings and the Ur River (Inya River tributary) in the Kemerovo region (southwestern Siberia, Russia). The Ursk tailings (consisting of sulfide and oxide wastes) and the down-gradient surface waters are good targets to study the distribution, speciation, and mobility of mercury (Hg^{2+}, CH_3Hg^+, HgS/HgSe) in a natural system affected by gold sulfide mining and refinement (e.g. cyanide leaching) operations. The mobility of mercury in natural waters depends on various geochemical conditions. In our case, natural organic matter in a swampy ravine at the Ursk site creates complexes with Hg, Au, Ag, Zn, and other elements (Lazareva et al. 2019; Myagkaya et al. 2016b, 2019; Saryg-ool et al. 2017). In addition, Hg mobility is affected by interaction with particulates (iron hydroxides) produced by the reaction of AMD with the Ur River water and the resulting pH and Eh changes in the river (Myagkaya et al. 2016a). This is the first examination of Hg behavior in aquatic systems and its natural and anthropogenic effects in this region.

Study Area

The Ursk tailings site, located at 54°27′11.03″ N, 85°24′09.76″ E near Ursk Village in Siberia, stores wastes left by cyanide leaching of pyritic and auriferous complex ores of the Novo-Ursk deposit in the Ur ore field of the northern Salair Ridge (Altai-Sayan Mountains). The Ur field belongs to one of seven large volcano-plutonic belts

and includes the Salair and Ur structures, which have many developed mines. The Novo-Ursk deposit of gold associated with pyrite, sphalerite, chalcopyrite, galena, arsenopyrite, tennantite, and cinnabar (Lazareva et al. 2019; Tokarev et al. 2004) was mined by open-cast operations about 90 years ago. Mercury was originally present in the ore as cinnabar (HgS) and fine Hg telluride (HgTe) and Hg selenide (HgSe) inclusions in pyrite and barite. Some mercury in pyrite occurs as an isomorphic impurity or as $HgCl_2$ and Hg^0 adsorbed on crystal defects (Gustaytis et al. 2010).

The sulfide-bearing waste rock at the Ursk site was dumped in two 10–12 m high piles of sulfide (wastes I) and oxide (wastes II) material, in the headwaters of a natural ravine (Gustaytis et al. 2010, 2013, 2018; Korzhuk et al. 2021; Myagkaya et al. 2013, 2016a, b, 2019; Saryg-ool et al. 2017). The main minerals in the waste rock dumps include barite, pyrite, and quartz in wastes I and quartz, barite, and jarosite, with sporadic gypsum and goethite, clay aluminosilicates, and less abundant pyrite in wastes II. The rock-forming minerals in the waste rock were previously characterized (Myagkaya et al. 2016a). Since 2011, the sulfide waste rock has been reprocessed to recover barite at a plant built by the OOO Barit company near a quarry that was formerly used to mine the Novo-Ursk sulfide deposit but was flooded when the mine was abandoned (quarry lake, location M3 in Fig. 1). Currently the lake receives no mine-influenced waters but rather serves as a water source for the processing plant. OOO Barit company diverted the wastewaters toward the dumps, the tailings, and the ravine.

Most of the sulfide waste rock has been reprocessed and the wastewater is being discharged into a creek that flows through the tailings to the Ur River, a tributary of the Inya River. Another historic mining site in the area remains in the Ur River valley where placer gold was dredged in the

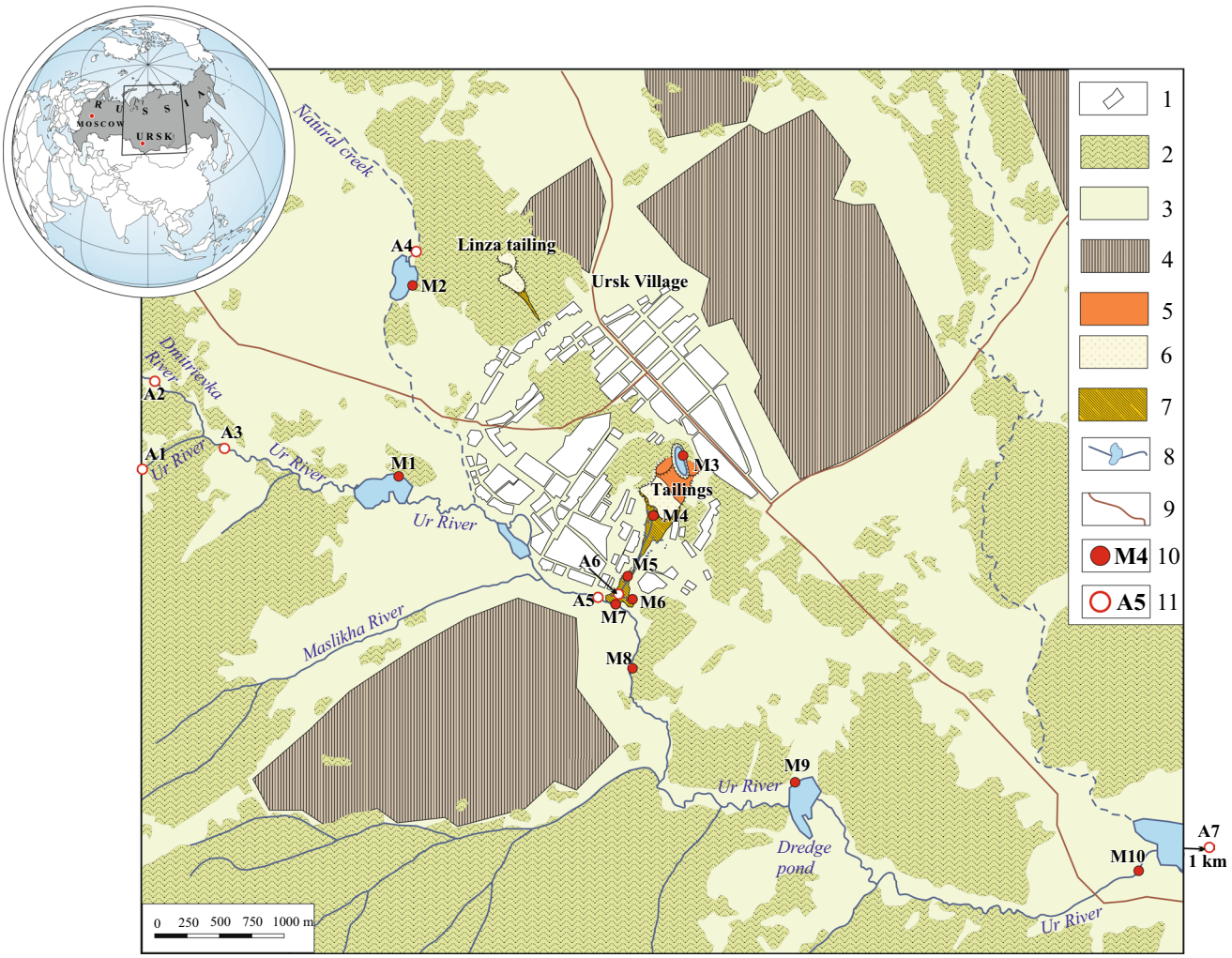

Fig. 1 Location of the Ursk gold mining area (54°27′11.03″ N, 85°24′09.76″ E) and sampling stations for natural waters and AMD around the Ursk tailings. Legend: 1 = Ursk Village; 2 = forest; 3 = meadow; 4 = cropland; 5 = waste rock dumps; 6 = tailings; 7 = swampy ravine of the tailings; 8 = rivers and ponds; 9 = roadways; 10 = monitoring stations; 11 = additional sampling stations of 2019

past. The dredging facilities included an impoundment of AMD supernatant that still exists near the former dumps and is about 600 m from the two dumps of sulfide and oxide wastes (location M6 in Fig. 1). The impoundment has reddish bottom sediments and is surrounded by piles of limestone gravel. Another pond remaining after placer gold sluicing is located 3 km downstream of the drainage creek input to the Ur River (dredge pond, location M9 in Fig. 1). The metal structures of the abandoned dredging site were only removed in 2018.

The creek that drains the Ursk tailings and flows into the Ur River is acidic (pH ≈ 2) due to interaction with the sulfide waste rock and consequently becomes an acid mine drainage (AMD) stream (locations M4-M5 in Fig. 1). Material in the two waste rock dumps, which are exposed to rainfall, spring floods, winds, and drainage, has been transported to the swampy ravine, which has remnants of decayed sedge and bulrush (peat mounds) and tree stumps. The degraded sedge mounds comprise natural organic matter that is buried under or is in places above the wastes. The swampy ravine of the tailings, 50–760 m by 250 m, consists of three zones; the middle zone (≈130 m from the waste rock dumps) is topographically divided into the western and eastern parts, which mainly include sulfide and oxide wastes, respectively. The area is heavily polluted (Gustaytis et al. 2010, 2018, 2021; Myagkaya et al. 2013, 2016a, b, 2019, 2021; Sarygool et al. 2017, 2020).

The climate in the area is continental, with long and cold winters and short and relatively warm summers. The winds are mostly from the southwest and south, at a mean annual speed of 1–6 m/s, with gusts of 25–30 m/s. The mean temperature of near-surface air in the warmest month (July) is + 18 °C over most of the site. The coldest month is January, when the mean temperature drops to –19.2 °C, with an absolute minimum of – 45 °C to – 48 °C. The warm season, with > 0 °C mean daily temperatures, usually lasts from about 10 April to 10 October, 175–195 days on average, including 96 frost-free days when air temperatures are consistently above 0 °C (Gustaytis et al. 2018).

Materials and Methods

Sampling and Sample Preparation

The surface waters in the Ursk area were sampled in several campaigns from 2007 to 2019 in summer months (June, July). Between 2007 and 2014, sampling was performed at 10 main monitoring stations (M1–M10 in Fig. 1) in the River Ur and its tributaries, as well as in the ponds, the quarry lake, and the AMD stream. The locations are shown in Fig. 1 and briefly described in Table 1. The impoundment of AMD supernatant (point M6) was only filled with water in 2009, 2011, and 2014. Stations M3 (quarry lake) and M4 (AMD) were only sampled in 2016. Additionally, several other stations (A1–A7, Fig. 1; Table 1) were sampled in 2019.

The sampling campaigns were conducted before and after the Barit processing plant began operating in 2011: in 2007, 2008, 2009 (stage I) and in 2011, 2012, 2014, 2016, and

Table 1 Sampling stations for AMD and natural waters not affected and affected by AMD in the swampy ravine of the Ursk tailings

Main station	Additional station	Location	
Natural waters (not affected by AMD)			
M1	A1, A3	Ur River (headwaters)	
–	A2	Dmitrievka River	
–	A4	A tributary of the Ur River	Natural creek
M2	–		Pond on natural creek
M3	–	Quarry lake (tailings site)	
–	A5	Ur River	
Acid mine drainage (AMD)			
M4	–	Headwaters of AMD (at dumps)	
M5	–	Middle part of AMD (0.5 km to dumps)	
–	A6	Lower part of AMD (0.7 km to dumps)	
M6	–	Impoundment of AMD supernatant (lower part of swampy ravine)	
Natural waters (affected by AMD)			
M7	–	AMD input into Ur River	
M8	–	Ur River at different distances to AMD	1 km
M9	–		3 km (dredge pond)
M10	–		5 km
–	A7		9 km

2019 (stage II), respectively. Furthermore, the campaigns of 2014, 2016, and 2019 postdated the onset of production from the Zvonchikha gold placer mine (2014) at the head of the natural creek flowing into the Ur River (M2 and A4 in Fig. 1, Table 1).

Mercury speciation in the water system was determined using the existing classification (Howe and Clark 2002; Wang et al. 2003), by successive filtering through 0.45 µm and 0.20 µm cellulose acetate membrane filters (*Sartorius Stedim*, Germany). The mercury species in the filter residue from the two steps were, respectively, suspended (0.45 µm filtrant residue) and colloidal (0.20 µm filtrant residue), while the final decanted solution (0.20 µm filtrate) contained operationally dissolved species only. The concentration of Hg in the dissolved + colloidal (Hg_{dc}) and suspended (Hg_{susp}) fractions were measured in all surface water samples collected in 2008, 2009, 2012, and 2014, while the 2019 samples were additionally analyzed for Hg in the dissolved (Hg_D) and colloidal (Hg_C) fractions. The total mercury concentration (Hg_{total}) in the water samples was analyzed in unfiltered samples from all campaigns, but was calculated as the sum of the respective fractions in the years when the Hg_{dc}, Hg_{susp}, Hg_D, and Hg_C mercury species were analyzed. The Hg_{total}, as well as Hg_{dc} and Hg_{susp}, data for stages I and II were averaged to better highlight the main trends.

The pH and oxidation–reduction potential (ORP) values of water samples were measured in situ using a portable Anion 7051 water analyzer (Infraspak-Analit, Russia) that allows no more than six-point calibration. In our case, the calibration was four-point, with standard buffer solutions of pH = 1.68, 4.01, 6.86, and 9.18 (State Standard 2004). The ORP values were corrected using the value of the standard hydrogen electrode (200 mV value was added to the measured ORP) as Eh. The instrument errors did not exceed ± 0.02 s.u. for pH and ± 2 mV for Eh.

Major ion chemistry (Na, Mg, K, Ca, Al, Fe cations, and HCO_3, SO_4, Cl, and NO_3 anions), as well as the concentrations of organic (TOC) and inorganic (TIC) carbon, were determined in unfiltered water samples collected in polypropylene test tubes. Pyrex borosilicate glass tubes were used for all samples for Hg analysis. Samples for the determination of cations and Hg in water were acidified with double-distilled HNO_3 (1 mL per 200 mL of water).

Preconditioning of Samples for Hg_{total}, Hg_{dc}, and Hg_D Measurements

Both unfiltered and filtered water samples for Hg assays were initially preconditioned using 1.5 mL of a 1:1 $H_2SO_4 + HNO_3$ mixture added to 50 mL of sampled water. Then the solution, with 3–4 drops of 5% $KMnO_4$, was left overnight; excess $KMnO_4$ was removed with 10% hydroxylamine-sulfate $(NH_2OH)_2 \cdot H_2SO_4$ added drop-by-drop until the solution became clear. Oxidation and extraction of mercury with $KMnO_4$ is commonly applied to environmental samples (Agemian and Chau 1976).

Analysis of Hg_{susp} and Hg_C Fractions

The technique applied for digestion and analysis of residue material on the filters (0.45 and 0.2 µm) was never described in our previous publications, but it is similar to the classical techniques used to determine Hg in soils and bottom sediments (Bock and Marr 1979). The residue on the filters was placed in a 100 mL conical vessel and digested in 5 mL of a 1:1 $HNO_3 + H_2SO_4$ mixture, heated to 75–80 °C on a water bath under a lid for 2–3 h, cooled to room temperature, heated again for 2–3 h, with 0.2 mL 5% $KMnO_4$, and left overnight. Excess $KMnO_4$ was removed with 10% hydroxylamine-sulfate $(NH_2OH)_2 \cdot H_2SO_4$ added drop-by-drop until the solution became clear; then, the solution was diluted with distilled water till a volume of 50 mL. The results were checked against standard bottom sediment samples of Baikal mud (BIL-1). The details of BIL-1, which is included in the Russian register of certified reference materials (CRM), were reported by Petrov et al. (1999).

Determination of Hg_R and Hg_{NR} in Particulate Matter

Reactive/non-reactive (or inorganic/organic) mercury can be determined in various ways (Bloom et al. 2003; Umezaki and Iwamoto 1971), by successively leaching groups of compounds at each step, as in the sequential leaching procedures (Bloom et al. 2003). In the absence of reliable chemical methods for separation of organic and inorganic mercury, we used the Hg_R vs. Hg_{NR} rather than organic vs. inorganic division (Lindqvist and Rodhe 1985).

The Hg_R and Hg_{NR} species were determined in particulates (suspended matter), bearing in mind that mercury can change from dissolved to particulate species and adsorb on or associate chemically with iron hydroxides and organic compounds present in surface waters. We modeled the reaction of AMD with particulates to see whether the latter can ensure secure immobilization of Hg. Reactive mercury species (Hg_R) were analyzed using the method of Umezaki and Iwamoto (1971), in first-filtered samples (0.45-µm) with added 10 mL 2 M H_2SO_4, which were heated to 75–80 °C in a water bath for 2–3 h and cooled down; then the solution was diluted with distilled water to a volume of 50 mL. The concentrations of Hg_{NR} were determined in second-filter samples (0.45-µm) digested in a 1:1 $HNO_3 + H_2SO_4$ mixture, from absorbance difference between Hg_{susp} and Hg_R after the flame atomic absorption spectroscopy (FAAS) assay.

Instrumentation

The anion composition of water samples was determined by capillary electrophoresis (CE) on a Kapel 103P instrument (Lumex, Russia). The detection limits ranged from 0.1 to 10 mg/L for different ions, and the accuracy was 15%.

Total organic carbon concentrations (TOC) were measured on an AG Multi N/C 2100S analyzer (Analytik Jena, Germany), which had an accuracy of 10% and a detection limit of 0.05 mg/L. The detection limit was estimated using blank samples (distilled water in test tubes similar to those used for field sampling of river and mine-influenced waters).

Cations in waters sampled in 2007–2016 were analyzed by FAAS. The FAAS assay was performed on a Solar M6 spectrometer with Zeeman and deuterium background correction systems (Thermo Electron, USA). The accuracy was 35% for element concentrations of 0.05 mg/L and ± 10% for higher concentrations up to 0.1 mg/L, at P = 0.95 confidence probability. The cations in the 2019 water samples were determined by inductively coupled plasma mass spectrometry (ICP-MS) on an Agilent 7500 spectrometer (Agilent Technologies, USA). The accuracy was 5% at $P = 0.95$.

The Hg concentration in the water samples and in the prepared solutions was measured by the cold vapor method, using $SnCl_2$ as a reducing agent, with subsequent FAAS assay on a RA-915 M analyzer with a RP-92 system (Lumex, Russia). The detection limit was 0.01 µg/L, and the accuracy was 20%.

The contents of Hg_R and Hg_{NR} were determined in the solid and recalculated by the volume of the filtered solution, so the detection limits were lower (about 0.001 µg/L).

Statistical Data Analysis

The processing of statistical data (mean, minimum and maximum values, and correlation coefficients) was carried out using Excel software and its data analysis package. The minimum, maximum, and mean Hg_{total}, Hg_{dc}, and Hg_{susp} were calculated over three measurements during stage I and five measurements at stage II.

The calculated correlation relationships and the significance of the coefficients were assessed by the Pearson test followed by comparison with Student's T test. The relationships were namely: (i) TOC/TIC and Fe/Al vs. Hg concentrations in fractions (Hg_C, Hg_D, Hg_{susp}) at N = 16 for AMD and natural waters (not affected and affected by AMD) and (ii) TOC/TIC vs. Hg_R and Hg_{NR} concentrations at N = 4 for natural waters not affected and affected by AMD.

Results

Major Ion Chemistry

The major ion chemistry of the natural water and wastewater bodies sampled in the summer months varied only slightly during the period of observation (2007–2019; Table 2). The water of the Ur River upstream of the AMD input (M1, Table 2) has a Mg–Ca–HCO_3 chemistry. The TDS, pH, and HCO_3 values decreased, while TOC increased with time (Table 1). The higher pH water of the pond on the natural creek (M2, Table 2) affected by the Zvonchikha mine had increased concentrations of HCO_3, K, Na, Mg, Ca, and Fe over time, while TOC concentrations decreased slightly.

The quarry lake (M3, Table 2) showed increasing concentrations in most of the measured parameters (pH, Eh, TDS, K, Na Mg, Ca, Fe, as well as all anions), which also became higher than in the Ur River; some values increased at least two-fold, and the pH increased from 7.9 to 8.7. Higher values of the parameters in 2019 may be due to water withdrawal for the OOO Barit operations, with the respective inputs of more alkaline groundwaters into the quarry (Table 2).

The AMD water chemistry beneath the tailings (M4, Table 2) changed with time relative to the results of 2007: in 2019, the pH increased by a factor of 1.8, whereas TDS values were decreased by a factor of 2.2. The AMD water chemistry changed from Al–Fe–SO_4 to Al–Ca–Mg–SO_4 type due to Ca–Mg increases and Fe–Al decreases. Sulfate concentrations likewise decreased by a factor of 2.5.

In the lower part of the AMD stream (M5, Table 2), the pH, TDS, SO_4, Fe, and Al values were similar to those in the headwaters (M4, Table 2). Only pH, TDS, Mg, and Al changed from 2007 to 2019, in the same way as at M4. The TOC concentration (Table 2) in the AMD stream decreased with distance from the tailings and time (by 2019), and is inversely proportional to pH (like TDS) in both cases. Lower-pH AMD waters can more easily remove organic matter from soil and peat material (Martynova 2011). Furthermore, dilution with wastewater from the Barit plant is also possible.

The impoundment samples (M6, Table 2) are of the Al–Fe-SO_4 type and are chemically similar to AMD (M4-M5, Table 2) but contain higher TOC concentrations, possibly due to dead leaves from birches growing around the M6 station.

The Ur River downstream of the AMD input (M7, Fig. 1) has higher solute concentrations than at the upstream locations (M1 and M2): TDS concentrations are 1.2–1.6 and 1.6–2.7 times higher, respectively. The increase was from 1.2 to 2.7 times in June 2011, in

Table 2 Characteristics of AMD and natural waters upstream and downstream of AMD input into the Ur River, sampled in three campaigns of July 2007, June 2011, and July 2019)

Parameter	Year	M1	M2	M3	M4	M5	M6	M7	M8	M9	M10
pH (s.u.)	2007	8.6	n.a	7.9	1.9	2.1	n.a	7.6	8.0	8.2	7.3
	2011	8.1	8.6	7.4	2.2	2.7	2.4	7.6	7.7	7.6	7.6
	2019	7.1	8.4	8.7	3.3	3.1	n.a	8.0	7.8	7.7	7.7
Eh, mV	2007	363	n.a	409	678	698	n.a	421	401	407	414
	2011	515	440	530	655	701	666	523	415	440	455
	2019	n.a	n.a	n.a	n.a	n.a	n.a	n.a	n.a	n.a	n.a
TDS, g/L	2007	0.43	n.a	n.a	5.7	n.a	n.a	0.40	0.40	0.35	0.34
	2011	0.34	0.16	0.21	5.0	4.4	3.2	0.42	0.36	0.24	0.32
	2019	0.30	0.30	0.35	2.6	2.5	n.a	0.47	0.46	0.47	0.46
Na, mg/L	2007	6.8	n.a	8.1	13	n.a	n.a	6.7	6.8	6.2	5.7
	2011	7.2	4.2	9.8	11	8.9	12	6.4	6.0	3.0	5.5
	2019	7.2	6.4	15	14	14	n.a	7.6	7.5	7.0	5.5
Mg, mg/L	2007	12	n.a	7.0	79	n.a	n.a	11	10.5	8.7	9.8
	2011	10	4.1	7.8	120	53	100	10	10	5.0	9.6
	2019	21	15	19	120	120	n.a	22	22.5	22	18
K, mg/L	2007	1.0	n.a	2.7	1.1	n.a	n.a	1.3	0.9	0.98	0.68
	2011	1.7	0.88	4.5	0.52	1.2	0.37	1.2	1.1	0.44	1.0
	2019	0.55	1.2	11	0.15	0.1	n.a	2.2	2.2	4.6	2.15
Ca, mg/L	2007	53	n.a	35	29	n.a	n.a	59	57	36	52
	2011	56	29	42	150	250	170	70	68	82	65
	2019	72	80	100	250	250	n.a	130	136	138	139
Al, mg/L	2007	0.09	n.a	0.03	250	n.a	n.a	1.5	0.10	0.09	0.04
	2011	0.05	0.05	0.05	277	90	230	0.05	0.32	0.19	0.25
	2019	0.02	0.01	0.02	18.5	20	n.a	0.11	0.13	0.02	0.01
Fe, mg/L	2007	0.3	n.a	0.03	770	n.a	n.a	0.02	0.07	0.22	0.06
	2011	0.01	0.02	0.01	870	57	690	0.01	0.01	0.01	0.04
	2019	0.14	0.07	0.14	277	280	n.a	0.21	0.17	0.19	0.17
HCO_3, mg/L	2007	340	n.a	n.a	5.0	5.0	n.a	290	305	290	260
	2011	250	100	66	4.2	6.3	0.5	260	230	130	201
	2019	186	172	95	25	0.5	n.a	285	260	270	280
SO_4, mg/L	2007	3.0	n.a	n.a	4500	810	n.a	12	7.6	2.6	2.0
	2011	14	16	63	3600	3390	1900	72	36	17	33
	2019	9.9	13	88	1830	1810	n.a	20	31	32	16.5
Cl, mg/L	2007	11	n.a	n.a	20	20	n.a	12	9.5	6.6	5.1
	2011	1.3	3.4	18	13	14	13	2.5	2.8	1.3	4.6
	2019	1.7	0.15	23	21	17	n.a	2.7	2.5	2.1	1.4
NO_3, mg/L	2007	4.5	n.a	n.a	n.a	n.a	n.a	n.a	n.a	1.6	4.7
	2011	n.a	n.a	n.a	n.a	n.a	n.a	n.a	n.a	n.a	n.a
	2019	0.5	0.15	2.0	20	14	n.a	1.3	1.3	0.15	0.15
TOC, mg/L	2007	n.a	n.a	n.a	n.a	n.a	n.a	n.a	n.a	n.a	n.a
	2011	5.7	12.7	5.9	14	9.5	10.5	4.0	5.0	5.6	5.6
	2019	8.5	9.6	6.0	5.7	6.3	n.a	5.4	5.7	7.2	5.4
Hg_{total}, µg/L	2007	0.02	n.a	0.28	16	7	n.a	0.12	0.40	0.17	0.12
	2011	0.02	0.02	n.a	39	15	5	n.a	n.a	n.a	0.03
	2019	n.a	0.32	0.32	40	25.8	n.a	1.5	0.65	0.10	0.16
Hg_{dc}, µg/L	2019	n.a	0.24	0.06	38	22	n.a	0.75	0.07	0.09	0.15
Hg_{susp}, µg/L	2019	n.a	0.08	0.27	1.6	3.5	n.a	0.71	0.58	0.01	0.01
Hg_R, µg/L	2012	0.016	n.a	0.006	0.42	0.09	n.a	0.02	n.a	n.a	0.004
Hg_{NR}, µg/L	2012	0.18	n.a	0.053	9.9	3.2	n.a	0.08	n.a	n.a	0.014

Each value in the table represents one sampling

AMD acid mine drainage, *s.u.* standard pH units, *n.a.* not analyzed, *TOC* total organic carbon, Hg_{dc} Hg in the dissolved + colloidal fraction, Hg_{susp} Hg in the suspended fraction, Hg_R reactive mercury species, Hg_{NR} non-reactive mercury species

Sampling locations are characterized in Table 1 and in Fig. 1

different water bodies in the Ur upper reaches, and by a factor of 1.6 in July 2019. The increase in the summer of 2011 was related to the beginning of the Barit reprocessing operations. The SO_4 concentrations were the highest in that year, but Al and Fe concentrations were near the minimum. The low Fe and Al concentrations may be due to the formation of Fe and Al hydroxide solids. Downstream of the AMD input, the major ion chemistry changed from Mg–Ca–HCO_3 to Mg–Ca–SO_4–HCO_3, and the SO_4 concentrations decreased with time. The trends from 2007 to 2019 (summer season) were: increased K, Na, Mg, Ca, SO_4, Fe, TOC, but decreased Al and Cl.

The Ur River water at 1, 3, and 5 km downstream of the AMD input (M8-M10, Table 2) is a Mg-Ca-HCO_3 type water. The contribution of SO_4 to the water chemistry became more noticeable after the OOO Barit operation started in summer of 2011 than it was before. The major ion chemistry of the Ur water at M8-M10 approached the upstream values (M1–M2) only in July 2007. After the summer of 2011, the water at any distance away from the AMD input had higher TDS, Ca, Al, HCO_3, SO_4, and Cl values, especially in 2019 (Table 2).

Hg Patterns in the Ur River—AMD System

The Hg_{total} concentrations in the Ur River and its tributary upstream of AMD (M1 and M2) before 2011 (stage I) were below or near detection (< 0.01 µg/L) and reached 0.03 µg/L only in May 2009. Values remained at that level after 2011 (stage II), in all years except July 2019 when Hg_{total} concentrations at M2 became more than 10 times higher (0.32 µg/L), which affected the average M1 + M2 value (Fig. 2). When Hg_{total} concentrations exceeded the detection limit, most of the mercury was transported in the dissolved + colloidal (Hg_{dc}) form: 72.8 and 75.5% of Hg_{total} during stages I and II, respectively (M1 + M2 in Fig. 2).

In the quarry lake (M3), the Hg_{total} concentrations were higher than in the Ur River; values were also higher before than after 2011 (Fig. 2). The fractionation likewise changed: Hg_{dc} predominated at stage I (0.16–0.59 µg/L, 36–96% of Hg_{total}, 65.8% on average) but decreased to 0.06–0.13 µg/L (20–30% of Hg_{total}) during stage II (Fig. 2, M3). The decrease may be due to water withdrawal for the Barit plant, which lowered water levels/volumes in the quarry lake. The withdrawn portion of water likely caused an increase in input to the quarry lake from lower-Hg groundwater. The pH in the lake increased from 7.1 (stage I) to 7.8 (stage II) and increased further to 8.7 in July 2019 (Table 2).

The AMD seeping from under the tailings (M4) showed the highest Hg_{total} values (Table 2; Figs. 1, 2): 11.4 to 16 µg/L in different years during stage I (average 13.2 µg/L) and 25.5 to 89 µg/L (48.8 µg/L on average) during stage II. The Hg_{dc} fraction was slightly higher than

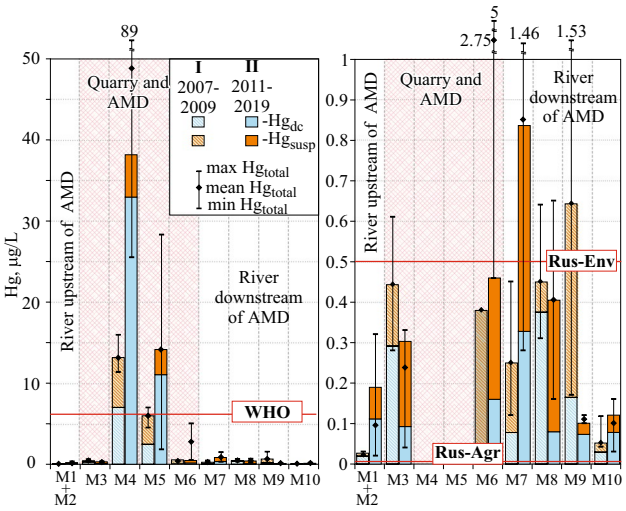

Fig. 2 Mercury concentrations (µg/L) in dissolved + colloidal (Hg_{dc}) and suspended (Hg_{susp}) fractions of surface waters and AMD of the Ursk tailings. Left and right panels show, respectively, data from all sampling stations and data without stations M4, M5 (immediate vicinity of AMD); total Hg concentrations (Hg_{total}) are quoted as maximum, minimum, and average values; WHO = guideline values of the World Health Organization (2017); Rus-Env = guideline values according to Russian Environment Health Criteria (Water Quality 2000); Rus-Agr = guideline values according to Decree 552 of the Ministry of Agriculture of the Russian Federation (Fishery Water Quality 2016); M1–M10 along *x* axis are sampling stations (see Fig. 1 and Table 1 for location IDs). Data for M6 at stage I refer to Hg_{total}

Hg_{susp} (7 vs 5 µg/L) and was 58% of Hg_{total} before 2011, but reached > 95% in July 2014 and July 2019; the percentages of the two fractions were equal only in August 2012 when Hg_{total} (25.5 µg/L) concentrations were the lowest. The operations of OOO Barit (including diverting the wastewaters toward the dumps, tailings, and ravine) likely led to mercury increase in AMD, especially Hg_{dc} (Fig. 2).

Samples from the AMD middle part (M5) contained notably lower concentrations of Hg_{total} than at M4: 4.5–7 µg/L (6.0 µg/L on average) during stage I and 1.8–25.8 µg/L (average 14 µg/L) during stage II (Figs. 1, 2). The fractionation changed from equal portions of Hg_{dc} and Hg_{susp} during stage I to a prevalence of Hg_{dc} at stage II (Fig. 2).

The impoundment samples (from M6) contained 0.38 µg/L Hg_{total} in May 2009, 5 µg/L in June 2011, and 0.46 µg/L in July 2014; the average over stage II was 2.7 µg/L (Figs. 1, 2), though the number of measurements at station M6 was insufficient to infer a statistically meaningful trend. The Hg_{total} values are much less than in AMD discharged into the impoundment (Fig. 2, M6). The fractions were analyzed only in July 2014, when up to 65% of mercury occurred in the suspended form (Hg_{susp}).

The Hg concentrations in the Ur river at the AMD input (M7) were higher than elsewhere in the river and increased

with time from 0.12 to 0.45 µg/L (average 0.25 µg/L) during stage I to 0.28–1.46 µg/L (0.85 µg/L on average) during stage II (Table 2; Figs. 1, 2). The Hg_{dc} fraction at stage I was relatively stable (0.13–0.16 µg/L), but the percentage varied, from 30 to 65%, as did the Hg_{susp} values (0.054–0.3 µg/L). The Hg_{dc} values at stage II varied from 0.084 to 0.75 µg/L and from 19.5 to 51.4%. The averaged values in the two periods were, respectively, 31 and 39%. Thus, although the total Hg concentration increased after 2011, much of it was bound to particulate matter and precipitated in the sediment as the river current is slow. The reaction of AMD with the river water produced ochreous phases (Fe and Al oxides and hydroxides, and various sulfate minerals), which can be easily mobilized during rainfalls and floods.

The average Hg_{total} concentrations in the Ur River 1 km downstream of AMD (M8, Figs. 1, 2) were 0.45 and 0.40 µg/L during stages I and II and ranged from 0.31–0.64 and 0.16–0.65 µg/L, respectively. However, the Hg_{dc} fraction was only 20% at stage I and increased to 83% (on average) during stage II.

The Ur River 3 km downstream of AMD (M9) contained ≤ 0.23 µg/L Hg_{total} in all years except in June 2008 (1.53 µg/L), which increased the average over stage I to 0.64 µg/L (Figs. 1, 2). In May 2009, the Hg_{dc} fraction was as high as 93% of the total value, but the high total Hg concentration in June 2008 was mainly due to the Hg_{susp} fraction (61%; 0.9 µg/L), although the Hg_{dc} value in June 2008 was likewise greater than in May 2009 (0.59 µg/L vs 0.21 µg/L). During stage II, the Hg_{total} concentrations ranged from 0.1 to 0.12 µg/L, with an average of 0.11 µg/L (Fig. 2), and Hg_{dc} predominated over Hg_{susp}.

The Hg_{total} concentrations in the Ur River 5 km downstream of the AMD input (M10, Figs. 1, 2) were higher than at M1 + M2 for the entire sampling period and averaged 0.052 µg/L and 0.1 µg/L during stages I and II, respectively (ranging from 0.04 to 0.12 µg/L and < 0.02–0.16 µg/L). The Hg_{dc} fraction predominated during both stages (Fig. 2, M10).

Mercury Fractionation and Speciation in the Ur—AMD System.

Dissolved, Colloidal, and Suspended Hg Fractions

The dissolved, colloidal, and suspended Hg fractions were studied in July 2019. The average Hg_{total} concentration in the middle reaches of the Ur River and its tributaries upstream of the AMD input (A1–A4, M2 in Figs. 1, 3) was 0.26 µg/L (0.1–0.37 µg/L), and the percentage of dissolved species (Hg_D) was 57%. The highest Hg_{total} and Hg_D values (0.37 and 0.25 µg/L) were recorded in the creek that drains the Zvonchikha gold placer area (Fig. 3, A4). The suspended fraction in the system was 32% of the total, while the colloidal fraction was only 11%. Near the AMD input (A5, Figs. 1, 3), Hg_{total} was 0.52 µg/L, and the suspended fraction was 61%. The area was quite strongly polluted with AMD judging by the Hg_{total} increase with respect to the concentrations in the Ur River (headwaters) and its tributaries (M1–M2, Table 2; A1–A4), as well as in the Ur River at different distances from the AMD (M8–M10, Table 2).

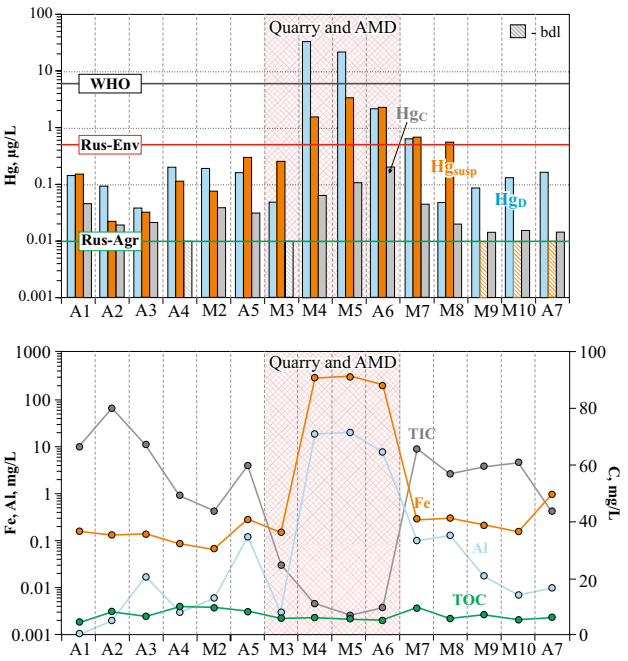

Fig. 3 Mercury concentrations (µg/L) in dissolved (Hg_D), colloidal (Hg_C), and suspended (Hg_{susp}) fractions in surface waters and AMD of the Ursk tailings, July 2019, vs. total organic carbon (TOC) and total inorganic carbon (TIC) concentrations, Fe, and Al (mg/L). WHO = guideline values of the World Health Organization (2017); Rus-Env = guideline values according to Russian Environment Health Criteria (Water Quality 2000); Rus-Agr = guideline values according to Decree 552 of the Ministry of Agriculture of the Russian Federation (Fishery Water Quality 2016); A1–A3 and M1–M10 along *x* axis are sampling stations (Table 1; Fig. 1)

In the quarry lake (M3, Figs. 1, 3), Hg_{total} was 0.32 µg/L; 84% was Hg_{susp}, 16% Hg_D, and Hg_C was below detection.

The highest Hg concentrations were in the AMD beneath the tailings, as in all previous years (M4, Figs. 1, 3), reaching 40 µg/L, with 95.5% Hg_D and 0.2% Hg_C. The middle segment of the AMD contained 25.8 µg/L of Hg_{total} (M5, Figs. 1, 3) and the lower part (A6, Figs. 1, 3) contained 5 µg/L, while the percentages of Hg_{susp} (13.6% at M5, 49% at A6) and Hg_C (0.43% at M5, 4.3% at A6) fractions increased.

Ur river water had the highest Hg_{total} concentrations (1.5 µg/L) at the AMD input (M7, Figs. 1, 3) in 2019 over the monitoring history, with almost equal Hg_D and Hg_{susp} percentages of 48 and 48.7%, respectively, and only 3% Hg_C. The Hg_{total} concentrations in the Ur River remained as high as 0.65 µg/L 1 km downstream of the AMD input (Figs. 1 and 3; M8), with 89% Hg_{susp} and 3% Hg_C. Farther

downstream at stations M9, M10, and A7 (Figs. 1, 3) Hg_{total} concentrations were lower (0.1–0.16 µg/L), at 78 to 87% Hg_D, while Hg_{susp} and Hg_C were below or near the detection limit, respectively. Therefore, the 2019 conditions were favorable for Hg transfer to particulate matter and its further precipitation to bottom sediment, with possible subsequent re-suspension during high flow.

Concentrations of C, Fe, and Al

The concentrations of total inorganic carbon (TIC) in surface water sampled in 2019 were different at all stations. In the Ur river, TIC values ranged from 60.5 to 72 mg/L upstream of AMD input (A1–A3, Fig. 3) and were slightly lower (50.2 mg/L on average) downstream of the input (M7–M10, A7, Fig. 3). The values in the natural creek and in the pond that receives wastewater from the Zvonchikha placer operation (A4, M2, Fig. 3) were twice as low as upstream. The TIC concentration in the Ur River immediately upstream of AMD input (A5, Fig. 3), where its influence is the greatest, was lower than at more upstream locations (A1–A3, Fig. 3). The TIC concentrations were also low in the quarry lake (Fig. 3, M3) and were the lowest in AMD itself (Fig. 3, M4, M5, M6).

The TOC concentration in the Ur River (headwaters) and the Dmitrievka River (A1–A3, Fig. 3) and in the wastewater from the Zvonchikha operation (4.2–8.3 mg/L; average 6.4 mg/L) was one tenth the TIC concentrations and was greater than the respective values in the creek and in the pond that received the Zvonchikha wastewater (A4, M2, Fig. 3). Generally comparable TOC values were measured in the AMD-quarry lake (Fig. 3) and the lower–upper Ur River, while TIC values were about eight times the TOC concentrations.

The TIC values showed an inverse correlation with the Hg_D, Hg_C, and Hg_{susp} fractions, with r values from − 0.67 to − 0.54 (at $\alpha = 0.05$). The correlation was the highest between Hg_{susp} and TIC ($r = -0.67$), given the variability in Eh, pH, and major ion chemistry.

Iron concentrations varied slightly in natural waters not affected by AMD (Fig. 3, A1–A4, M2), increased immediately upstream of the AMD input to the river (Fig. 3, A5), and were notably higher downstream of the AMD input (Fig. 3, M6-M10, A7). Elevated Fe concentrations were also observed in the quarry lake and were at least three orders of magnitude higher in the AMD itself (Fig. 3, M4, M5).

Aluminum concentrations were below 0.01 mg/L in natural waters not affected by AMD (Fig. 3, A1–A4, M2), with the exception of A3, increased before the AMD input (Fig. 3, A5), and became still higher downstream (M6–M10, A7, Fig. 3); the values never attained the background over the sampled segment of the river. The Al concentrations were low in the quarry lake (Fig. 3, M3) and exceeded 10 mg/L in AMD (Fig. 3, M4, M5). Both Fe and Al correlated with mercury at $r = 0.7$–0.91 and $r = 0.59$–0.93, respectively ($\alpha = 0.05$). The correlation coefficients increased in the series Hg_C – Hg_D – Hg_{susp} for Fe and Hg_C – Hg_{susp} – Hg_D for Al.

Reactive and Non-reactive Hg Species

The particulate matter in all water samples from the area generally contains greater amounts of non-reactive than reactive Hg species (Table 2). Note that the use of H_2SO_4 in experiments, which is much stronger than the AMD at the Ursk tailings, may lead to partial dissolution of the stable Hg species (e.g. HgS cinnabar and metacinnabarite, as well as HgSe) that are soluble only in aqua regia (Bloom et al. 2003). Although the bulk concentrations of Hg_{susp} ($Hg_{NR} + Hg_R$ total) in the Ur downstream of AMD (Fig. 4a, Table 2, M7, M10) were within the background (Table 2, M1), the Hg fractions in the particulate matter remained stable, while the percentage of Hg_R increased. The correlation of Hg_R and Hg_{NR} with carbon (TOC and TIC) was significant only for the TOC – Hg_{NR} pair ($r = 0.97$; $\alpha = 0.01$) in the Ur River samples (Fig. 4b), both upstream and downstream of the AMD input.

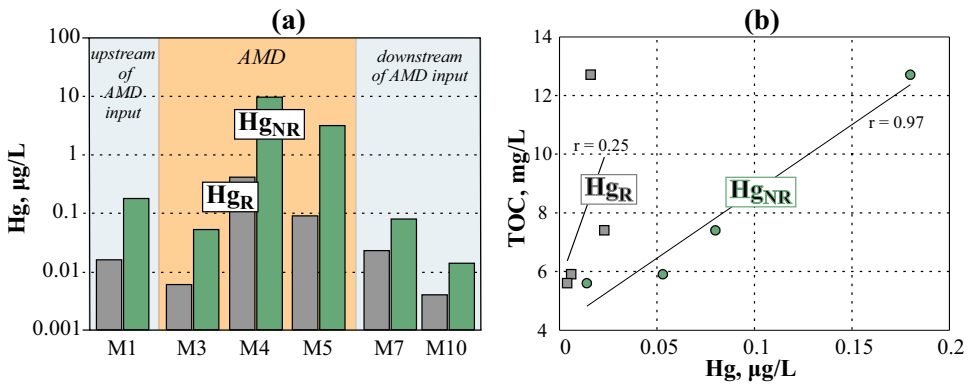

Fig. 4 **a** Reactive (Hg_R) and non-reactive (Hg_{NR}) mercury in particulate matter (µg/L) from AMD and natural waters upstream and downstream of AMD input into the Ur River; **b** TOC-Hg_R and TOC-Hg_{NR} correlations in natural waters. For sampling locations see Table 1 and Fig. 1. Squares and circles in panel (**b**) refer, respectively, to reactive and non-reactive mercury species

Discussion

Variability in Concentration of Hg_{total} and Other Elements

The natural average total mercury (Hg_{total}) concentration in the world's unpolluted rivers ranges from 0.001 to 0.005 µg/L (Leopold et al. 2010), but local concentrations can be much higher because of a high natural background (Table 3). The concentration of Hg_{total} in the Ur River before it receives the AMD drainage from the Ursk tailings ranged from 0.02 to 0.32 µg/L, which is up to 100 times the maximum global background average for pristine river settings (Table 3). The markedly increased Hg concentrations in the river upstream of the AMD may

Table 3 Hg_{total}, Hg_{dc} and Hg_{susp} concentrations in natural and mine-influenced waters worldwide

Location		Hg_{total}, µg/L	Hg_{dc}, µg/L	Hg_{susp}, µg/L	References
Natural Waters					
Rivers worldwide		0.001–0.005	No data	No data	Leopold et al. (2010)
Rivers upstream of Xunyang Hg mining area (Shaanxi Province China)		0.012–0.081	0.007–0.038	0.005–0.04	Qiu et al. (2012)
Idrija River and tributaries, upstream of Idrija Hg Mine (Idrija Hg province, Slovenia)		0.0002–0.041	0.00005–0.01	0.0001–0.037	Kocman et al. (2011)
Paglia River, upstream of Abbadia San Salvatore Mine (Monte Amiata Hg province, Southern Tuscany, Italy)		0.0032	No data	No data	Rimondi et al. (2012)
West Siberia (Russia)	Rivers in southern Kuznetsk coal basin	No data	0.13	No data	Malikova et al. (2011)
	Ur River upstream of AMD, 2007 (M1)	0.02	No Data	No data	*Our data*
	Ur River upstream of AMD, 2019 (M2)	0.32	0.24	0.08	
	Ob River	No data	0.0006	50	Coquery et al. (1995)
West Siberia/East Siberia boundary (Russia)	Yenisei River	No data	0.0003	50	Coquery et al. (1995)
East Siberia (Russia)	Selenga River basin	≤0.01	No data	No data	Roberts et al. (2020)
	Lake Baikal	≤0.003			
	Lake Baikal tributaries	No data	0.01–0.06	No data	Malikova et al. (2011)
	Lena	No data	0.0011	120	Coquery et al. (1995)
Russian Far East	Primoriye region[a]	0.0005–0.048	0.0005–0.003	0.0002–0.014	Shulkin and Ivlev (2013)
Mine-influenced waters					
Rivers downstream of Xunyang Hg mining area (Shaanxi Province China)		0.0089–23.5	0.0075–0.23	0.00014–23.4	Qiu et al. (2012)
Valdeazogues River (Almaden Hg province, Spain)		0.11–20.3	No data	No data	Berzas Nevado et al. (2003)
Paglia River, downstream of Abbadia San Salvatore Mine (Monte Amiata Hg province, Italy)		0.004–1.4	No data	No data	Rimondi et al. (2012)
Idrija River and tributaries, downstream of Idrija Hg Mine (Idrija Hg province, Slovenia)		0.0007–0.71	0.0002–0.14	0.0004–0.7	Kocman et al. (2011)
Carson River (Sierra Nevada gold-silver region, USA)		0.004–2.1	0.002–0.046	0.002–2.05	Bonzongo et al. (1996)
Russia	Ur River downstream of AMD, 2007 (M7–M10)	0.12–0.4	No data	No data	*Our data*
	Ur River downstream of AMD, 2019 (M7–M10)	0.10–1.5	0.07–0.75	0.01–0.71	
AMD					
Coast Range Hg mineral belt (California, USA)		8–450	3.7–10	4.3–440	Rytuba 2000
New Idrija Hg Mine (California, USA)		0.005–0.42	No data	No data	Ganguli et al. (2000)
Russia	AMD from Ursk tailings, 2007 (M4–M5)	7–16	No data	No data	*Our data*
	AMD from Ursk tailings, 2019 (M4–M5)	25.8–40	22.3–38.4	1.6–3.5	

[a]Hg range in rivers from different areas in the Primoriye region (Russian Far East)

have two causes: either the started gold production from the Zvonchikha placer mine and the related wastewater discharge into the creek (M2), or forest fires in the summer of 2019 in the Irkutsk region. The smoke of the 2019 fires reached the sampling area, and mercury is known to be able to migrate far from fire sources (Scherbov and Lazareva 2010). However, the Hg_{total} concentrations measured in the Ur River upstream of the AMD input are comparable with those reported for Hg provinces worldwide (Table 3), such as Shaanxi Province in China, with the Xunyang Hg mining area (Qiu et al. 2012); central Spain, with the Almaden Hg area (Berzas Nevado et al. 2003; Schmid et al. 2013); the Monte Amiata Hg province in southern Tuscany, Italy (Rimondi et al. 2012); and the Idrija Hg province in Slovenia (Cerovac et al. 2018; Hines et al. 2000; Kocman et al. 2011), etc. (Shevyrev 2013). The Ursk study area belongs to the Altai-Sayan mercury province in the Salair Ridge, which has a generally high geochemical background as it comprises seven volcano-plutonic belts that host mercury-bearing sulfide deposits (Lazareva et al. 2019). The province consists of the Kurai, Salair, Altai-Kuznetsk, and Sayan zones and displays multiple natural Hg anomalies associated with large fault systems (Kuznetsov 1963, 1976).

The AMD and natural water samples in the Ur River network have major ion patterns similar to those in other sulfide mines tailings, including Hg provinces (Fig. 5). Note that the composition of AMD in different mining areas worldwide varies broadly depending on the composition and water content of the mine wastes, local geomorphology (Nieva et al. 2018; Schaider et al. 2014), climate (air temperature and precipitation), altitude, and microbial activity (Akcil and Koldas 2006). Generally, the AMD from many mining sites is rich in sulfate and iron and

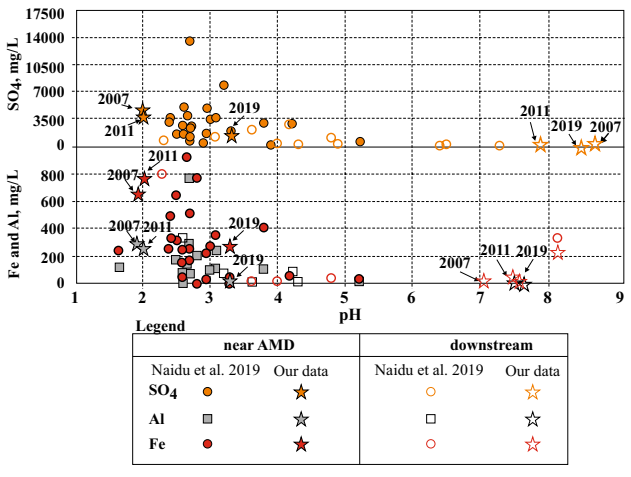

Fig. 5 pH dependence of SO_4, Fe, and Al concentrations in water samples collected at different distances to AMD input into the Ur River

has quite a low pH of 1.7–8.1, 3.6 on average (n = 45), or 1.7–4.0 (average 2.9 over n = 34) exclusive of high values from 4.0 to 8.1 (Naidu et al. 2019; Fig. 6). The low pH enhances the ability of AMD to leach metals from tailings and other wastes and rocks and thus increases solute concentrations (Naidu et al. 2019). Higher-pH water samples generally have lower metal concentrations because of dilution with natural waters and the precipitation of Fe/Al oxides-hydroxides upon mixing of AMD with natural waters (Bigham 1994; Bigham et al. 1996; Gas'kova et al. 2007; Murray et al. 2014; Seal and Hammarstrom 2003), though some sulfate, Fe, and Al typically remain dissolved (Naidu et al. 2019).

The Hg_{total} concentrations were highest in the AMD headwaters (M4) and middle part (M5) and became 2.5 and 3.7 times higher in 2019 than in 2007 (reprocessing of the wastes began in 2011; Table 2). Compared to the sampling results from other Hg provinces (Table 3), the Hg_{total} concentrations in the Ursk AMD are intermediate between those in the New Idrija Hg Mine (California, USA) and the Coast Range Hg mineral belt (California, USA), and significantly decrease (depending on year, Table 2) downstream (from M4 to M5). Mercury and other elements can bind to the ochreous phases, including jarosite, K-jarosite, schwertmannite, and goethite, which precipitate from pH < 3 solutions containing > 3000 mg/L SO_4 (Bigham 1994; Bigham et al. 1996). Jarosite can accommodate Hg as ½ Hg^{2+} in site A (Dutrizac and Jambor 2000), while schwertmannite and goethite have a high sorption capacity for certain metals (Pb, Cu, Zn, Cd) (Murray et al. 2014; Seal and Hammarstrom 2000) and can also scavenge some Hg (Gustaytis et al. 2010). Therefore, the Hg_{total} decreases in AMD away from the tailings (from M4 to M5 and partly to M6), which may be due to co-precipitation and adsorption of elements with secondary minerals that form at higher pH. This inference is consistent with the observed SO_4 patterns. As shown previously (Gustaytis et al. 2017), new Hg minerals (sulfides and selenides) can form in the organic-rich bottom sediment of the impoundment (M6).

The Hg concentrations in AMD are sensitive to climate factors. For instance, Hg_{total} concentrations in AMD were the highest in April during snow melting, when wastes were shed rapidly from the dumps (Gustaytis et al. 2018). Furthermore, enrichment can occur in cold weather by the so-called cryo-concentration effect as a result of solution freezing or buffering (Lacelle et al. 2007; Ethier et al. 2012). In spring, quite high concentrations of Hg, Al, Fe, Cu, Zn, and Pb, above those in the AMD (Gustaytis et al. 2014; Myagkaya et al. 2014), were measured in a stream of melted snow flowing through the tailings ravine covered by oxide wastes. On the other hand, hot weather in the summer (up to 30–35 ºC, 19.7 ºC on average), can concentrate saline sulfate solutions and stimulate microbial activity (Vonk et al. 2015), leading to further leaching from the wastes.

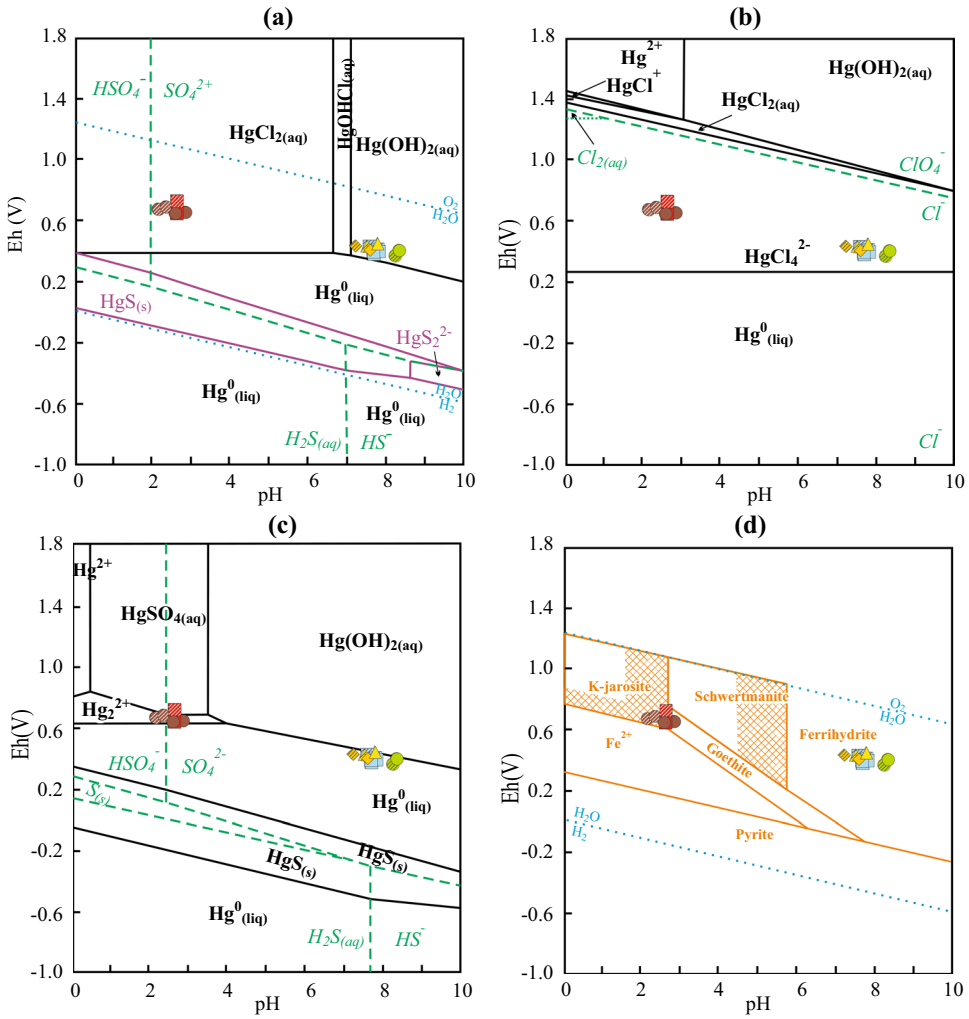

Fig. 6 Samples of natural surface waters and AMD mine waters in the Ursk tailings and the enclosing areas plotted on Pourbaix diagrams. **a** Hg–S–Cl–H_2O stable system at 298 K with activities for dissolved species of Hg = 10^{-9} M, S = 10^{-4} M and Cl = $10^{-4.5}$ M (Andersson 1979); **b** Hg–Cl–H_2O stable system at 298 K with activities of dissolved Hg and chloride of 10^{-6} and 1 M (Brandon et al. 2001); **c** Hg–S–H_2O stable system at 298 K with activities of dissolved Hg and sulfur of 10^{-6} and 1 M (Brandon et al. 2001); **d** Fe-S-H_2O system (hatching shows metastable zone) (Bigham et al. 1996). $Hg^0_{(liq)}$ = uncharged liquid metal Hg; subscripts at Hg: (aq) = aqueous and (s) = solid Hg species. Hatched symbols refer to stage I (2007–2009); plain symbols refer to stage II (2011–2019). Colored dashed and dotted lines refer to different species of S (**a**, **c**), H_2O (**a**, **d**), and Cl (**b**); solid lines refer to species of Hg (**a**–**c**) and Fe (**d**); *green circle* = natural waters not affected by AMD (M1 + M2); yellow triangle = quarry lake (M3); brown circle = AMD (M4, M5); red square = impoundment of AMD supernatant (M6); orange diamond = AMD input into the Ur River (M7); blue square = Ur River 1–5 km downstream of AMD input into the Ur River (M8–M10)

High Hg_{total} concentrations in the Ur River downstream of AMD may be due additionally to partial re-suspension of sorbed elements from sediments. Re-suspension results from electrostatic interactions on the surface of mineral particles (Sarkar et al. 1999) and breakdown of weak bonds (Cossa et al. 2001; Laurier et al. 2003; Mataba et al. 2016; Tseng et al. 2001). The probability of such a process in the Ur River is supported by the fact that the Hg concentrations in suspended matter are higher downstream of AMD.

Hg_{total} Patterns and Water Quality Guidelines

The concentrations of Hg_{total} in the Ur River upstream of the AMD input (M1; M2; Table 2; Fig. 2) never exceeded the guideline value of 6 µg/L recommended for inorganic mercury by the World Health Organization (2017) nor the maximum permissible limits for drinking, household, and recreation water uses according to the Russian environmental health criteria (Rus-Env = 0.5 µg/L; Water Quality 2000, 2007). Although in 2019 Hg_{total} concentrations in Ur River

upstream of the AMD input reached 32 times the Rus-Agr limit (0.01 µg/L) for Fishery Water Quality (2016), local people still fish in that stretch of the Ur River.

The Hg concentrations in the quarry lake (Fig. 2, M3), where local people swim and fish, did not exceed the WHO guidelines (World Health Organization 2017) but exceeded the Rus-Agr level recommended for fishery (Fishery Water Quality 2016) for the whole period of observations and were above the Rus-Env limit (Water Quality 2000, 2007) in 2009.

The Hg_{total} concentrations in the AMD ((Fig. 2, M4, M5) were orders of magnitude in excess of all three guideline values (though these waters would not be used for drinking) and were 38–500 times the Rus-Agr values in the impoundment (M6, Fig. 2).

The Hg_{total} concentrations in the Ur River at the AMD input (M7; Fig. 2) exceeded the WHO guideline value in stage I and the Rus-Env limit in stage II. The Hg concentrations in the Ur River 1 km downstream of the AMD input (M8, Fig. 2) exceeded the Rus-Env standard in 2008 and the Rus-Agr standard from 2007 through 2019. The average and maximum values in the Ur River 5 km downstream of AMD at M10 (Fig. 2) exceeded only the Rus-Agr level.

Mercury Fractions

The study area is located in the western part of the Kuznetsk coal basin, and rivers in the southern part of the basin generally have high concentrations of dissolved mercury Hg_{dc} (Malikova et al. 2011, Table 3). The relative concentrations of dissolved (+colloidal) and suspended mercury fractions in the Ur-AMD system change from $Hg_{susp} < Hg_{dc}$ in the samples from the Ur River and its tributaries upstream of AMD (M2, Fig. 2, and A1–A4 Fig. 3), as well as in the AMD samples near the tailings (M4, Fig. 2, 3) and in the middle AMD segment (M5, Fig. 2, 3), to $Hg_{susp} > Hg_{dc}$ in the impoundment samples (M6, Fig. 2), in the Ur River before the AMD input (A6, Fig. 3), as well as downstream of this input (M7-M8, Fig. 2, 3).

In natural surface waters in Hg mining areas, Hg commonly occurs in particulate matter, and the Hg_{susp} component exceeds the Hg_{dc} (Telmer et al. 2006) because of the tendency for Hg to be adsorbed on particle surfaces (Ullrich et al. 2001). The average Hg_{susp} concentration in limited samples from Russia's rivers and lakes is 0.23 µg/L, while Hg_{dc} is only 0.09 µg/L (Petrosyan 1999). The respective concentrations of Hg_{dc} and Hg_{susp} in Siberian rivers are shown in Table 3 (Coquery et al. 1995) and the average values may reach 74 µg/L Hg_{susp} and 0.0007 µg/L Hg_{dc}. Note though that Coquery et al. (1995) apparently overestimated the Hg_{susp} concentration, because the average Hg_{total} concentration in the Ob River (between the Tom' and Irtysh river mouths) was reported (Savichev 2003) to be only 0.11 µg/L (data for 1990–2002). The percentages of Hg_{susp} relative to Hg_{total} in the Zhutong River, together with tributaries of other rivers (Gongguan, Shu, River Xun, Qianyou, etc.), in the Xunyang Hg mining area (Shaanxi Province, China), at pH 7.6–9.5, were in the 35–95% range (65.6% on average), whereas the Hg_{dc} percentages range from 5 to 65%; the respective concentrations range from 0.06 to 9.3 µg/L Hg_{susp} and 0.00021–3.5 µg/L Hg_{dc}. Most often, the Hg_{susp} fraction dominates when total Hg concentrations are high (Zhang et al. 2009).

The grain size and composition of the suspended matter control the Hg enrichment (Savenko 2006). The partitioning of Hg between the solution and the colloid depends on the content of dissolved carbon, Fe, and Al, i.e. the main components of the colloid-forming systems (Pokrovsky and Schott 2002). There are two hypotheses concerning the composition of colloidal particles: (i) inorganic and organic colloids are most often bound to one another (Gu et al. 1995; Koskinen and Harper 1990) and to Fe oxyhydroxides; (ii) colloids consist either of iron hydroxides or of organic compounds, while Al and Fe mainly form inorganic colloids (aluminosilicates and/or metal oxyhydroxides) not bound to organic compounds (Pokrovsky and Schott 2002).

The increase of Hg_{susp} concentrations in AMD away from the Ursk tailings correlates with increasing percentages of particulate matter and higher pH values that cause the precipitation of ochreous phases. In addition to the latter process, dilution of AMD in the Ur River may produce organic-mineral colloids or Fe and Al oxyhydroxides (Gu et al. 1995; Koskinen and Harper 1990) due to the formation of $Fe(OH)_3$ and $Al(OH)_3$ and interaction with organic components (Kulmatov et al. 1985; Stevenson 1994).

Mercury Speciation

The aqueous speciation of mercury and its mobilization/immobilization under different conditions can be examined using geochemical modeling and Pourbaix (Eh–pH) diagrams (Lusilao-Makiese et al. 2013; Navarro et al. 2009; Pestana et al. 2000). In oxidized environments, Hg(II) can form complexes with $C1^-$ ($HgCl^+$ and $HgCl_{2(aq)}$) in aerated waters with low pH (up to 7); $HgClOH_{(aq)}$ and $Hg(OH)_{2(aq)}$ complexes can exist at neutral and basic pH values, respectively. In reduced environments, Hg(II) has a high affinity with sulfide and forms insoluble $HgS_{(s)}$ (Davis et al. 1997) or $Hg^0_{(liq)}$ (Fitzgerald et al. 2007). Mercury is rarely present as free Hg^{2+} in aqueous solutions because of its affinity for sorption onto solid particles and complexation, especially with chlorides and organic ligands (Schuster 1991; Wallschläger et al. 1998a, b). Mercury complexes with organic ligands are stable under reduced conditions over a large range of pH values (Tromans et al. 1996). The adsorption of Hg cations on clay minerals, oxides, and organic compounds

depends on pH (Biester et al. 1999): Hg(I) is unstable in aqueous solutions at neutral pH, unlike Hg(II), but occurs as Hg_2^{2+} in low-pH environments where it can disproportionate to Hg(II) or $Hg^0_{(liq)}$ in the presence of OH^-, F^-, or CN^- (Davis et al. 1997).

For example, most of the mercury in the Camaqua river basin (southern Brazil) with pH 5.8–7.1 and Eh 70–254 mV occurs as $Hg^0_{(liq)}$, which explains its relatively low mobility (Pestana et al. 2000). In southeastern Spain, Hg mineralization consists of low-sulfidation epithermal hot-spring deposits in the Betic Ranges (e.g. Valle del Azogue Mine). As shown by equilibrium speciation modeling using data from two old mines (Navarro et al. 2009), the main Hg species in solutions that modeled rainwater and reacted with the wastes can be $Hg^0_{(liq)}$ and $Hg(OH)_{2(aq)}$ for the Bayarque Mine (pH 8.3, Eh 59 mV, Hg 0.8 µg/L), and also $HgCl_{2(aq)}$, $HgCl_3^-$ and $HgClOH_{(aq)}$ for the Valle del Azogue Mine (pH 7.4–8.1, Eh from − 60 to 219 mV, Hg from 716 to > 2000 µg/L) due to high concentrations of Hg and chloride. However, Navarro et al. (2009) note that errors in Eh and pH may lead to deviation from the real conditions used as inputs to geochemical models. The pH dependence of Hg speciation was also reported from the West Rand region (Gauteng, South Africa) for the case of the Randfontein waters, with average and maximum Hg_{total} of 0.05 µg/L and 0.22 µg/L, respectively, and with pH values ranging from 2.9 to 5 and Eh values ranging from 260 to 620 mV (Lusilao-Makiese et al. 2013); these waters contain mercury mostly as $Hg^0_{(liq)}$ at pH 5–8 and as $HgCl_{2(aq)}$ at pH 2–3. Possible Hg species predicted by geochemical modeling (Lusilao-Makiese et al. 2013) were $HgCl_x^{+2-x}$, Hg^{2+} and $HgClOH_{(aq)}$, as well as $HgSO_{4(aq)}$ in water with a pH of 2.9 (mining area), and $Hg(OH)_{2(aq)}$, $HgCl_x^{+2-x}$ and $HgClOH_{(aq)}$ in pH 3.1 water (hunting area). Lusilao-Makiese et al. (2013) used these modeling results to infer that pH increases may lead to removal of dissolved Hg from water as $Hg^0_{(liq)}$ and $Hg(OH)_{2(aq)}$, or as $HgS_{(s)}$ in low-Eh conditions, which reduces the mobility and toxicity of mercury.

The Hg concentration trends in the AMD-Ur River system can be illustrated by plotting the data from the Ursk area from stages I and II on Pourbaix diagrams (Fig. 6) for the stable systems Hg–S–Cl–H_2O (Andersson 1979), Hg–Cl–H_2O and Hg-S-H_2O (Brandon et al. 2001), as well as for the system Fe–S–H_2O. Below we discuss first the Hg species in AMD (M4–M5) and impoundment (M6) samples and then those in natural waters not affected and affected by AMD. The calculations for the system Hg–S–Cl–H_2O (Fig. 6a) show that main Hg species in mining-related waters (AMD and impoundment, M4–M6) is $HgCl_{2(aq)}$ (Andersson 1979), for the whole observation period. The complex $HgCl_4^{2-}$ can be expected to dominate in wastewater samples (Fig. 6b), according to the calculations for Hg–Cl–H_2O (Brandon et al. 2001), and chloride complexes may be responsible for higher Hg concentrations in Cl-rich AMD (Table 2) than in natural waters. On the other hand, natural waters may have lower Hg inputs or be diluted. However, the sampled wastewaters also contained less abundant Hg(I) – Hg_2^{2+} species, which predominated in AMD for the whole observation period, as shown in the Hg-S-H_2O diagram (Fig. 6c), where the Hg(I)–Hg_2^{2+} species has a small stability field next to the fields of Hg and $HgSO_{4(aq)}$. Furthermore, thiosulfate complexes, such as $Hg(SO_3)_2^{2-}$, can control Hg mobility under metastable conditions (Brandon et al. 2001). Such complexes may exist in AMD and reach significant percentages. The pH-Eh values in the Ursk AMD vary both in space (away from the tailings) and in time (stages I and II). The Hg_2^{2+} stability field is very narrow, and Eh–pH changes may markedly affect Hg mobility. The AMD sample close to the tailings (Fig. 6c, M4–M5) is predicted to be in the Hg_2^{2+} field; acidic samples away from the tailings such as impoundment (M6, Fig. 6c) were within the stability field of $HgSO_{4(aq)}$ in stage I but remained within the stability field of Hg_2^{2+} in stage II. Furthermore, the pH and Eh values of the AMD samples (brown circles and red squares) fell within the stability field of jarosite during stage I but were at the stability margins of other Fe minerals and within the goethite stability field for sample M5 during stage II (Fig. 6d). Thermodynamic modeling for sulfide tailings of the Berikul processing plant (Gas'kova et al. 2007) predicted several steps of oxidation leaching and formation of secondary Al and Fe minerals: alunite–jarosite–goethite (from early goethite to a late stable phase), which is consistent with the series jarosite–schwertmannite–ferrihydrite–goethite of Bigham (1994). The possibility for Hg to incorporate isomorphically into site A in the structure of jarosite-group minerals ($AFe_3(SO_4)_3(OH)_6$, where A is H_3O^+, Na^+, K^+, Ag^+, ½ Pb^{2+} or ½ Hg^{2+}) was shown for Hg-jarosite synthesized in the laboratory (Dutrizac and Jambor 2000). The concentrations of Hg_{total} in the AMD samples (M-4–M-5, Table 2) increased during stage II, while measured Eh–pH values showed the samples moving to the goethite stability field. Thus, the Hg mobility could depend on the formation of jarosite, and the potential for Hg to be incorporated into the mineral.

Calculations for the system Hg–Cl–H_2O (Fig. 6b) predict that $HgCl_4^{2-}$ can be a dominant Hg species in the natural waters of the Ursk area as well (quarry lake and Ur River upstream and downstream of AMD), which does not contradict the data on Hg speciation in aerated neutral pH water (Davis et al. 1997; Lusilao-Makiese et al. 2013). The calculated results for the systems Hg–S–Cl–H_2O (Fig. 6a) and Hg–S–H_2O (Fig. 6c) show that the Ursk natural waters plot close to the line that divides the $Hg^0_{(liq)}$ and $Hg(OH)_{2(aq)}$ stability fields. This may be evidence that the dividing line traces the species change in potential-forming element(s). Similar results were reported, for instance, for hot springs in the Uzon caldera (Dobretsov et al. 2015). Either $Hg^0_{(liq)}$ or

$Hg(OH)_{2(aq)}$ species dominate in different diagrams of Fig. 6: $Hg(OH)_{2(aq)}$ in panel *a* and $Hg^0_{(liq)}$ in panel *c*, which agrees with modeling showing that either $Hg^0_{(liq)}$ or $Hg(OH)_{2(aq)}$ may prevail in neutral-pH environments (Andersson 1979; Davis et al. 1997; Lusilao-Makiese et al. 2013; Navarro et al. 2009; Pestana et al. 2000). However, much of the Hg is expected to occur as charged organic complexes, $HgH_{-1}L^{-1}$ (L stands for the organic component of the ligand; chemical structure unstated). This inference stems from calculations of Tromans et al. (1996), given the organic enrichment of the local natural waters (Table 2) and their Eh–pH values, which correspond to the stability of ferrihydrite and can result in sorption of Hg (Fig. 6d).

Reactive and Non-reactive Mercury Species

Our results, with reference to published geochemical modeling data (Andersson 1979; Brandon et al. 2001; Lusilao-Makiese et al. 2013; Navarro et al. 2009; Pestana et al. 2000), show that the 'Ur River-AMD' system may contain the following Hg species and compounds: $HgCl_{2(aq)}$, $Hg(OH)_{2(aq)}$, Hg^{2+}, $Hg^0_{(liq)}$, $Hg(SO_3)_2^{2-}$, $HgSO_{4(aq)}$ (as impurity in jarosite), and $HgH_{-1}L^{-1}$. $HgCl_2$ is soluble in deionized water (Bloom et al. 2003) and is thus a reactive species (Hg_R). Other reactive Hg species include Hg^{2+}, which can be adsorbed by OH groups on the surfaces of compounds (Walcarius et al. 1999); metallic $Hg^0_{(liq)}$ (Ganguli et al. 2000); $HgH_{-1}L^{-1}$ (Tromans et al. 1996); HgX_2, HgX_3^-, and HgX_4^{2-} ($X = Cl^-, OH^-, Br^-$); HgC_2O_4; and Hg^{2+} complexes with organic acids (Lindqvist and Rodhe 1985). The non-reactive species (Hg_{NR}) include $HgSO_{4(aq)}$ and, possibly, $HgS_{(s)}$ and CH_3Hg^+, which Lindqvist and Rodhe (1985) classified as reactive species. Furthermore, Hg^{2+} can form a stable complex with thiol (mercaptan) groups (Beckers and Rinklebe 2017), which is the main complex associated with Hg transport in water systems (Ullrich et al. 2001) and is insoluble at acidic pH (Bloom et al. 2003). Most Hg_{NR} species originate from minerals and compounds common to the natural organic matter of the swampy ravine in the Ursk tailings: HgS (cinnabar), m-HgS (metacinnabar), HgSe (tiemmanite), Hg sulfohalides corresponding to perrudite ($Ag_4Hg_5S_5(I,Br)_2Cl_2$), and minor Hg components in primary pyrite (Myagkaya et al. 2016b, 2017, 2020; Saryg-ool et al. 2017). These Hg minerals are poorly soluble in water and weak acids (Bloom et al. 2003; Mikac et al. 2002); HgS (cinnabar and metacinnabarite) or HgSe can dissolve only in aqua regia (Bloom et al. 2003). Thus, they are likely to be stable in AMD. Mercury migration as Hg minerals in suspension was also reported from other Hg provinces (Beckers and Rinklebe 2017; Ganguli et al. 2000).

The percentage of reactive species in the Hg_{susp} component from the Ur River samples upstream of the AMD was 8–10%, while the AMD samples contained only 2.8–4.1% Hg_{susp}, although the Hg concentrations were high. The percentage of Hg_{susp} increased to 22% downstream of the AMD input, while the Hg_R fraction increased, possibly due to the increasing Hg^{2+} that co-precipitated with and was sorbed by secondary ochreous phases (Dutrizac and Jambor 2000; Murray et al. 2014; Seal and Hammarstrom 2000). We have observed no correlation between Hg_R and TOC, i.e. the amount of $HgH_{-1}L^{-1}$ complexes was minor, but the Hg_{susp} concentrations in the natural waters up- and downstream of the AMD input, as well as the Hg_{NR} concentrations, correlate with TOC (Fig. 4b). Therefore, Hg in the particulate matter is most likely bound to insoluble organic components from the Ur River and to primary mineral particles (e.g. pyrite from ores) and secondary minerals (jarosite group).

Mercury in the Ur River, both up- and downstream of the AMD, can exist as methylmercury because fulvic and humic acids are sources of methyl groups. Methylation is possible at pH 6–8 for humic acid and pH 0–12 for fulvic acid, at Eh > 0.5 mV, and in the presence of organic matter (Ullrich et al. 2001). Note that interactions of Hg with humic substances may lead to Hg^{2+} reduction to $Hg^0_{(liq)}$ in water systems, which decreases the total amount of dissolved Hg (Ullrich et al. 2007). Conditions for the methylation reaction (Ullrich et al. 2001) exist all along the Ur River, judging by the TOC and Hg concentrations (Table 2) and the correlation of TOC (Fig. 4b) with Hg_{NR} (including CH_3Hg^+). The extremely high toxicity of CH_3Hg^+ (World Health Organization 1990) poses risks to aquatic life and fish consumption. Organic carbon was also present in the AMD (M4 and M5; Table 2), but does not correlate with Hg_{NR} (though Hg_{total} was highest in the AMD), and most of the Hg in particulate matter migrates with mineral particles, which makes methylation in the AMD unlikely. Mining in the Salair region led to Hg increases in the system both upstream (gold production from the Zvonchikh placer) and downstream (Eh–pH change) of the AMD input to the Ur River, as well as in the AMD itself.

Currently, mine wastes are attracting much attention worldwide as a potential source of useful components. With the technological advances in the recovery of metals, the former wastes could potentially be considered ores. However, reprocessing requires special caution and responsibility. It must be preceded by geochemical characterization and laboratory test work, because remining may trigger releases of toxic elements to the environment.

Summary and Conclusions

The study of Hg concentrations, fractions, and aqueous speciation in the Ur River system and its tributaries interacting with AMD in the area of the Ursk sulfide tailings (Salair Ridge area, Altai-Sayan mercury province) from 2007

through 2019, before the onset of reprocesssing operations at the Barit Plant in 2011 (stage I: 2007, 2008, and 2009) and after 2011 (stage II: 2011, 2012, 2014, 2016, and 2019), led to the following conclusions:

1. Reprocessing of cyanide wastes of the Novo-Ursk sulfide gold deposit (Ursk tailings) by the OOO Barit Company since 2011 has changed the composition of the AMD and caused TDS decreases from 5.7 to 2.5–2.6 and a pH increase from 1.9–2.1 to 3.1–3.3. Discharge of wastewaters into the AMD stream led to a flow rate increase, and major cations and TDS in the Ur River sampled downstream of the AMD input were greater than upstream of this input, especially in 2011.
2. The natural Hg_{total} concentrations in the Ur River upstream of the AMD input were quite high (0.02–0.32 µg/L) due to the Altai-Sayan Hg province's high geochemical background. The surface water system is being additionally loaded by ongoing mining and processing operations, including gold production from the Zvonchikha placer since 2013–2014 and reprocessing of dumped wastes at the Ursk tailings site. The Hg_{total} concentrations in the AMD ranged from 7 to 40 µg/L for the observation period. The Ur River downstream of the AMD input contains much more Hg than the non-affected water upstream of it (0.1–1.5 µg/L).
3. The mercury enrichment (Hg_{total} concentrations) in the AMD source was about three times greater during monitoring stage II than during stage I. The Hg concentration in AMD decreased by a factor of 1.5–2.5 away from the tailings. The high Hg concentrations at the source may have been associated with slightly elevated pH values that hindered the precipitation of jarosite (which can bind Hg as an isomorphic impurity), whereby the Hg in the source waters remained mobile.
4. Mercury in the Ur River and in the AMD occurs primarily in Hg_{dc} and Hg_{susp} fractions. The Hg_{dc} fraction dominates over Hg_{susp} upstream of the AMD input, whereas more Hg is transported with suspended matter downstream of the AMD input ($Hg_{susp} > Hg_{dc}$). In the AMD stream, the fractionation changed from equal amounts of Hg_{dc} and Hg_{susp} during stage I to prevalent Hg_{dc} at stage II.
5. Mercury in water behaves in reactive and non-reactive ways. The percentage of Hg_{NR} is higher than Hg_R in the particulates of the Ur River and in the AMD samples. Stable Hg compounds are expected to be present largely as organic complexes, including CH_3Hg^+, judging by the correlation of Hg_{NR} with TOC in the Ur River both up- and downstream of the AMD. The high Hg_{NR} concentrations in the AMD samples are due to primary and secondary Hg minerals (HgS, m-HgS, HgSe, jarosite, etc.). Reactive mercury may occur as $Hg^0_{(liq)}$, $Hg(OH)_{2(aq)}$, and $HgCl_{2(aq)}$ species or as Hg^{2+} adsorbed to OH groups on mineral surfaces.
6. Long-term monitoring of the 'AMD – Ur River' system, with a focus on Hg behavior and speciation то есть (dissolved, colloidal, and suspended), reveals that Hg contamination of the Ur River has occurred since initial mining and reprocessing of the sulfide tailings. The tailings will remain unstable and hazardous long after reprocessing. Consequently, environmental studies should have been conducted prior to the mining and the onset of the reprocessing operations to prevent further pollution, especially with Hg.
7. The reported results have important implications for Hg pollution from mining and processing activities in natural river ecosystems with varying environmental and geochemical conditions (pH, Eh, TOC, temperature, etc.). These results are of interest for comparative analysis of Hg migration in similar aquatic ecosystems exposed to anthropogenic releases and in provinces with naturally elevated Hg background concentrations.

Acknowledgements We wish to thank PhD Zh.O. Badmaeva for analytical work (Hg determination) and PhD B.L. Shcherbov, I.S. Kirichenko, and N.V. Ishchuk for assistance in the field. The fieldwork and some geochemical analyses were performed on a government assignment to the V.S. Sobolev Institute of Geology and Mineralogy at the Analytical Center for Multi-Elemental and Isotope Research (Novosibirsk, Russia). The 2019 samples were collected and analyzed with the support of the Russian Science Foundation, Project 18-77-10056. The manuscript profited much from the thoughtful criticism of the reviewers and editors.

References

Agemian H, Chau ASY (1976) An improved digestion method for the extraction of mercury from environmental samples. Analyst 101(1199):91–95

Akcil A, Koldas S (2006) Acid mine drainage (AMD): causes, treatment and case studies. J Clean Prod 14(12–13):1139–1145. https://doi.org/10.1016/j.jclepro.2004.09.006

Al TA, Leybourne MI, Maprani AC, MacQuarrie KT, Dalziel JA, Fox D, Yeats PA (2006) Effects of acid-sulfate weathering and cyanide-containing gold tailings on the transport and fate of mercury and other metals in Gossan Creek: Murray Brook mine, New Brunswick, Canada. Appl Geochem 21(11):1969–1985. https://doi.org/10.1016/j.apgeochem.2006.08.013

Andersson A (1979) The biogeochemistry of mercury in the environment. Elsevier/North-Hoiland Biomedical Press, New York City

Baldi F, Parati F, Filippelli M (1995) Dimethylmercury and dimethylmercury-sulfide of microbial origin in the biogeochemical cycle of Hg. Water Air Soil Pollut 80:805–815

Bavec S, Biester H, Glosar M (2014) Urban sediment contamination in former Hg mining district, Idrija, Slovenia. Environ Geochem Health 36(3):427–439. https://doi.org/10.1007/s10653-013-9571-6

Beckers F, Rinklebe J (2017) Cycling of mercury in the environment: sources, fate, and human health implications: a review. Crit Rev

Environ Sci Technol 47(9):693–794. https://doi.org/10.1080/10643389.2017.1326277

Berzas Nevado JN, García LB, Rodríguez RMD (2003) Distribution of mercury in the aquatic environment at Almade, Spain. Environ Pollut 122:261–271. https://doi.org/10.1016/S0269-7491(02)00290-7

Biester H, Gosar M, Müller G (1999) Mercury speciation in tailings of the Idrija mercury mine. J Geochem Explor 65(3):195–204. https://doi.org/10.1016/S0375-6742(99)00027-8

Bigham JM (1994) Mineralogy of ochre deposits formed by sulfide oxidation. In: Jambor JL, Blowes DW (eds) Environmental Geochemistry of Sulfide Mine-Wastes, Short Course Series, vol 22. Waterloo, Mineralogical Assoc of Canada, pp 103–132

Bigham JM, Schwertmann U, Traina SJ, Winland RL, Wolf M (1996) Schwertmannite and the chemical modeling of iron in acid sulfate waters. Geochim Cosmochim Act 60(12):2111–2121. https://doi.org/10.1016/0016-7037(96)00091-9

Bloom NS, Preus E, Katon J, Hiltner M (2003) Selective extractions to assess the biogeochemically relevant fractionation of inorganic mercury in sediments and soils. Anal Chim Acta 479(2):233–248. https://doi.org/10.1016/S0003-2670(02)01550-7

Bock R, Marr IL (1979) A handbook of decomposition methods in analytical chemistry. International Textbook Company, p 444

Bonzongo JCJ, Heim KJ, Warwick JJ, Lyons WB (1996) Mercury levels in surface waters of the Carson River-Lahontan Reservoir system, Nevada: influence of historic mining activities. Environ Pollut 92(2):193–201. https://doi.org/10.1016/0269-7491(95)00102-6

Bonzongo JCJ, Nemer BW, Lyons WB (2006) Hydrologic controls on water chemistry and mercury biotransformation in a closed river system: the Carson River, Nevada. Appl Geochem 21(11):1999–2009. https://doi.org/10.1016/j.apgeochem.2006.08.010

Boulet MP, Larocque AC (1998) A comparative mineralogical and geochemical study of sulfide mine tailings at two sites in New Mexico, USA. Environ Geol 33(2–3):130–142

Brandon NP, Francis PA, Jeffrey J, Kelsall GH, Yin Q (2001) Thermodynamics and electrochemical behavior of Hg–S–Cl–H_2O systems. J Electroanal Chem 497(1–2):18–32. https://doi.org/10.1016/S0022-0728(00)00445-9

Branfierun BA, Bishop K, Roulet NT, Granberg G, Nilsson M (2001) Mercury cycling in boreal ecosystems: the long-term effect of acid rain constituents on peatland pore water methylmercury concentrations. Geophys Res Lett 28:1227–1230. https://doi.org/10.1029/2000GL011867

Cerovac A, Covelli S, Emili A, Pavoni E, Petranich E, Gregoric A, Urbanc J, Zavagno E, Zini L (2018) Mercury in the unconfined aquifer of the Isonzo/Soča River alluvial plain downstream from the Idrija mining area. Chemosphere 195:749–761. https://doi.org/10.1016/j.chemosphere.2017.12.105

Coquery M, Cossa D, Martin JM (1995) The distribution of dissolved and particulate mercury in three Siberian estuaries and adjacent Arctic coastal waters. Water Air Soil Pollut 80(1–4):653–664

Cossa D, Elbaz-Poulichet F, Nieto JM (2001) Mercury in the Tinto-Odiel estuarine system (Gulf of Cádiz, Spain): sources and dispersion. Aquat Geochem 7(1):1–12

Davis A, Bloom NS, Que Hee SS (1997) The environmental geochemistry and bioaccessibility of mercury in soils and sediments: a review. Risk Anal 17(5):557–569. https://doi.org/10.1111/j.1539-6924.1997.tb00897.x

Dobretsov NL, Lazareva EV, Zhmodik SM, Bryanskaya AV, Morozova VV, Tikunova NV, Chebykin EP (2015) Geological, hydrogeochemical, and microbiological characteristics of the oil site of the Uzon caldera (Kamchatka). Russ Geol Geophys 56(1–2):39–63. https://doi.org/10.1016/j.rgg.2015.01.003

Dobrovolsky VV (2004) Role of soil organic matter in migration of heavy metals. Priroda 7(2004):35–39 (**in Russian**)

Dutrizac JE, Jambor JL (2000) Jarosites and their application in hydrometallurgy. Rev Mineral Geochem 40(1):405–452. https://doi.org/10.2138/rmg.2000.40.8

Dutta M, Islam N, Rabha S, Narzary B, Bordoloi M, Saikia D, Silva LFO, Saikia BK (2020) Acid mine drainage in an Indian high-sulfur coal mining area: cytotoxicity assay and remediation study. J Hazard Mater 389:121851. https://doi.org/10.1016/j.jhazmat.2019.121851

Ethier MP, Bussière B, Benzaazoua M, Garneau P (2012) Effect of temperature on the weathering of various waste rock types from the Raglan Mine. J Cold Reg Eng. https://doi.org/10.1061/9780784412473.079

Ferrari CP, Moreau AL, Boutron CF (2000) Clean conditions for the determination of ultra-low levels of mercury in ice and snow samples. Fresenius J Anal Chem 366(5):433–437

Fishery Water Quality (2016) Maximum Permissible Level of Pollutants in Lakes and Rivers Used for Fishery. Decree no. 552 of 13 Dec. 2016. Ministry of Agriculture of the Russian Federation, Moscow (**in Russian**)

Fitzgerald WF, Lamborg CH, Hammerschmidt CR (2007) Marine biogeochemical cycling of mercury. Chem Rev 107:641–662. https://doi.org/10.1021/cr050353m

Galán E, Gómez-Ariza JL, González I, Fernández-Caliani JC, Morales E, Giráldez I (2003) Heavy metal partitioning in river sediments severely polluted by acid mine drainage in the Iberian Pyrite Belt. Appl Geochem 18(3):409–421. https://doi.org/10.1016/S0883-2927(02)00092-6

Ganguli PM, Mason RP, Abu-Saba KE, Anderson RS, Flegal AR (2000) Mercury speciation in drainage from the New Idria mercury mine. Calif Environ Sci Techn 34(22):4773–4779. https://doi.org/10.1021/es991364y

Gas'kova OL, Bortnikova SB, Shironosova GP, (2007) Processes of chemical weathering of minerals in sulfide-bearing tailing dumps: modeling of the composition of vadose water and secondary phases. Chem Sustain Dev 3:333–346 (**in Russian**)

Gilmour CC, Henry EA, Mitchell R (1992) Sulfate stimulation of mercury methylation in freshwater sediments. Environ Sci Technol 26:2281–2287. https://doi.org/10.1021/es00035a029

Gu B, Schmitt J, Chen Z, Liang L, McCarthy JF (1995) Adsorption and desorption of different organic matter fractions on iron oxide. Geochim Cosmochim Acta 59(2):219–229. https://doi.org/10.1016/0016-7037(94)00282-Q

Gustaytis MA, Lazareva EV, Bogush AA, Shuvaeva OV, Shcherbakova IN, Polyakova EV, Badmaeva ZhO, Anoshin GN (2010) Distribution of mercury and its species in the zone of sulphide tailing. Dokl Earth Sci 432(2):778–782. https://doi.org/10.1134/S1028334X10060152

Gustaytis MA, Lazareva EV, Myagkaya IN, Bogush AA, Shuvaeva OV (2013) Mercury species in solid matter of dispersion of the Ursk tailing dispersion train (Ursk village, Kemerovo region, Russia). In: E3S Web Conf 1: 19007–19011. DOI: https://doi.org/10.1051/e3sconf/20130119007

Gustaytis MA, Myagkaya IN, Chumbaev AS (2014) Migration of mercury with snowmelt water into the river network around the dispersion train of tailings: case study of the Novo-Ursk deposit of complex ore (Kemerovo region). In: Proc, VII Young-Carrier Siberian Conf, with International Participation, Novosibirsk State Univ, Novosibirsk (**in Russian**)

Gustaytis MA, Myagkaya IN, Shcherbov BL, Lazareva EV (2016) Mercury pollution after operations at the Novo-Ursk gold deposit (Kemerovo region). Bull Irkutsk State Univ Earth Sci 18:14–24 (**in Russian**)

Gustaytis MA, Myagkaya IN, Saryg-ool BYu, Lazareva EV (2017) Mercury patterns in bottom sediments in the area of the Ursk tailings (Kemerovo region). Bull VGU Ser Geol 4:114–122 (**in Russian**)

Gustaytis MA, Myagkaya IN, Chumbaev AS (2018) Hg in snow cover and snowmelt waters in high-sulfide tailing regions (Ursk tailing dump site, Kemerovo region, Russia). Chemosphere 202:446–459. https://doi.org/10.1016/j.chemosphere.2018.03.076

Gustaytis MA, Myagkaya IN, Malov VI, Lazareva EV, Shuvaeva OV (2021) Mercury speciation in natural and mining-related systems. J Sib Fed Univ Biol Chem 14(2):184–196. https://doi.org/10.17516/1998-2836-0227

Gutiérrez-Mosquera H, Marrugo-Negrete J, Díez S, Morales-Mira G, Montoya-Jaramillo LJ, Jonathan MP (2021) Mercury distribution in different environmental matrices in aquatic systems of abandoned gold mines, western Colombia: focus on human health. J Haz Mat 404(A):124080. https://doi.org/10.1016/j.jhazmat.2020.124080

Hesterberg D, Chou JW, Hutchison KJ, Sayers DE (2001) Bonding of Hg (II) to reduced organic sulfur in humic acid as affected by S/Hg ratio. Environ Sci Technol 35(13):2741–2745. https://doi.org/10.1021/es001960o

Hines ME, Horvat M, Faganeli J, Bonzongo JCJ, Barkay T, Major EB, Scott KJ, Bailey EA, Warwick JJ, Lyons WB (2000) Mercury biogeochemistry in the Idrija River, Slovenia, from above the mine into the Gulf of Trieste. Environ Res 83(2):129–139. https://doi.org/10.1006/enrs.2000.4052

Howe KJ, Clark MM (2002) Fouling of microfiltration and ultrafiltration membranes by natural waters. Environ Sci Technol 36(16):3571–3576. https://doi.org/10.1021/es025587r

Jaliehvand F, Leung BO, Izadifard M, Damain E (2006) Mercury (II) cysteine complexes in alkaline aqueous solution. Inorg Chem 45:66–73. https://doi.org/10.1021/ic0508932

Kim CS, Rytuba JJ, Brown GE Jr (2004) Geological and anthropogenic factors influencing mercury speciation in mine wastes: an EXAFS spectroscopy study. Appl Geochem 19(3):379–393. https://doi.org/10.1016/S0883-2927(03)00147-1

Kocman D, Kanduč T, Ogrinc N, Horvat M (2011) Distribution and partitioning of mercury in a river catchment impacted by former mercury mining activity. Biogeochemistry 104(1–3):183–201

Korzhuk AV, Myagkaya IN, Rozanov AS, Ershov NI, Saryg-ool BYu, Malov VI, Gustaytis MA, Shipova AA, Lazareva EV, Peltek SE (2021) Metagenomics data of microbial communities of natural organic matter from the dispersion train of sulfide tailings. Data Brief 35:106720. https://doi.org/10.1016/j.dib.2021.106720

Koskinen WC, Harper SS (1990) The retention process: mechanisms. In: Cheng (ed) Pesticides in the Soil Environment: Processes, Impacts and Modeling vol 2, pp 51–77. DOI: https://doi.org/10.2136/sssabookser2.c3

Kõszegi-Szalai H, Paál TL (1999) Equilibrium studies of mercury (II) complexes with penicillamine. Talanta 48(2):393–402. https://doi.org/10.1016/S0039-9140(98)00258-6

Kulmatov RA, Rakkhmatov U, Kist AA, Savenko VS (1985) Thermodynamic state of Hg, Cd, and Zn in the surface waters of the arid zone in the USRR. Doklady AN SSSR 272(5):1226–1228 (**in Russian**)

Kuznetsov VA (1963) Tectonic division and main features of magmatism-related metallogeny in Gorny Altai. Geology and Metallogeny of Gorny Altay, Izd, O AN SSSR, Novosibirsk, pp 6–68 (**in Russian**)

Kuznetsov VA (1976) Genetic groups, ores, and mineral types of mercury deposits. In: Smirnov VI, Kuznetsov VA, Fedorchuk VP (eds) Metallogeny of mercury. Nedra, Moscow, pp 7–12 (**in Russian**)

La Colla NS, Botté SE, Marcovecchio JE (2019) Mercury cycling and bioaccumulation in a changing coastal system: From water to aquatic organisms. Mar Pollut Bull 140:40–50. https://doi.org/10.1016/j.marpolbul.2018.12.051

Lacelle D, Doucet A, Clark ID, Lauriol B (2007) Acid drainage generation and seasonal recycling in disturbed permafrost near Eagle Plains, northern Yukon Territory, Canada. Chem Geol 243(1–2):157–177. https://doi.org/10.1016/j.chemgeo.2007.05.021

Laperdina TG (2000) Determination of mercury in natural waters. Nauka, Novosibirsk (**in Russian**)

Laurier FJG, Cossa D, Gonzalez JL, Breviere E, Sarazin G (2003) Mercury transformations and exchanges in a high turbidity estuary: the role of organic matter and amorphous oxyhydroxides. Geochim Cosmochim Acta 67(18):3329–3345. https://doi.org/10.1016/S0016-7037(03)00081-4

Lazareva EV, Tsimbalist VG, Shuvaeva OV (2002) Arsenic speciation in the tailings impoundment of a gold recovery plant. Geochem Explor Environ Anal 2(3):263–268. https://doi.org/10.1144/1467-787302-030

Lazareva EV, Myagkaya IN, Kirichenko IS, Gustaytis MA, Zhmodik SM (2019) Interaction of natural organic matter with acid mine drainage: in-situ accumulation of elements. Sci Tot Environ 660:468–483. https://doi.org/10.1016/j.scitotenv.2018.12.467

Leopold K, Foulkes M, Worsfold P (2010) Methods for the determination and speciation of mercury in natural waters—a review. Anal Chim Acta 663(2):127–138. https://doi.org/10.1016/j.aca.2010.01.048

Leung BO, Jalilehvand F, Mah V (2007) Mercury (II) penicillamine complex formation in alkaline aqueous solution. Dalton Trans 41:4666–4674

Lindqvist O, Rodhe H (1985) Atmospheric mercury – a review. Tellus B 37(3):136–159. https://doi.org/10.1111/j.1600-0889.1985.tb00062.x

Liu F, Niu L, Chen H, Li P, Tian F, Yang Q (2017) Seasonal changes of polycyclic aromatic hydrocarbons in response to hydrology and anthropogenic activities in the Pearl River estuary, China. Mar Pollut Bull 117(1–2):255–263. https://doi.org/10.1016/j.marpolbul.2017.01.061

Lusilao-Makiese JG, Cukrowska EM, Tessier E, Amouroux D, Weiersbye I (2013) The impact of post gold mining on mercury pollution in the West Rand region, Gauteng, South Africa. J Geochem Explor 134:111–119. https://doi.org/10.1016/j.gexplo.2013.08.010

Malikova IN, Anoshin GN, Badmaeva ZO (2011) Mobile mercury species in soils of natural and natural-technogenic landscapes. Russ Geol Geophys 52(3):320–332. https://doi.org/10.1016/j.rgg.2011.02.005

Martynova NA (2011) Soil chemistry: soil organic matter. A Manuel. Irkutsk State Univ, Irkutsk (**in Russian**)

Mataba GR, Verhaert V, Blust R, Bervoets L (2016) Distribution of trace elements in the aquatic ecosystem of the Thigithe river and the fish Labeo victorianus in Tanzania and possible risks for human consumption. Sci Tot Environ 547:48–59. https://doi.org/10.1016/j.scitotenv.2015.12.123

Mikac N, Foucher D, Niessen S, Fischer JC (2002) Extractability of HgS (cinnabar and metacinnabar) by hydrochloric acid. Anal Bioanal Chem 374(6):1028–1033

Murray J, Kirschbaum A, Dold B, Guimaraes EM, Miner EP (2014) Jarosite versus soluble iron-sulfate formation and their role in acid mine drainage formation at the Pan de Azúcar mine tailings (Zn-Pb-Ag), NW Argentina. Minerals 4(2):477–502. https://doi.org/10.3390/min4020477

Myagkaya IN, Lazareva EV, Gustaitis MA, Zayakina SB, Polyakova EV, Zhmodik SM (2013) Gold in the sulfide waste-peat bog system as a behavior model in geological processes. Dokl Earth Sci 453(1):1132–1136. https://doi.org/10.1134/S1028334X13110135

Myagkaya IN, Gustaytis MA, Chumbaev AS (2014) Seasonal variations of Au and Ag in mining-related waters in the area of the Ursk Tailings (Kemerovo region). In: Proc, VII Young Carrier Conf on Earth Sciences 17–21 Nov. 2014, Novosibirsk: 305–306 (**in Russian**)

Myagkaya IN, Lazareva EV, Gustaytis MA, Zhmodik SM (2016a) Gold and silver in a system of sulfide tailings. Part 1: migration in water flow. J Geochem Explor 160:16–30. https://doi.org/10.1016/j.gexplo.2015.10.004

Myagkaya IN, Lazareva EV, Gustaytis MA, Zhmodik SM (2016b) Gold and silver in a system of sulfide tailings. Part 2: reprecipitation on natural peat. J Geochem Explor 165:8–22. https://doi.org/10.1016/j.gexplo.2016.01.016

Myagkaya IN, Saryg-ool BY, Lazareva EV, Ishchuk NV, Zhmodik SM (2017) Gold and silver speciation in the Novo-Ursk mineraldeposit. In: Metallogeny of past and present oceans – 2017. Classification of mineral deposits and causes of diversity. XXIII Young Carrier Seminar with International Participation, 24-28 April 2017, IMin UrO RAN, Miass, Bull. vol 23. pp. 171–176. (**In Russian**)

Myagkaya IN, Gustaytis MA, Kirichenko IS, Saryg-ool BYu, Lazareva EV (2019) Acid mine drainage contamination of the Ur impoundment. In: Environ Geochem E3S Web Conf 98: 09021. DOI: https://doi.org/10.1051/e3sconf/20199809021

Myagkaya IN, Lazareva EV, Zaikovskii VI, Zhmodik SM (2020) Interaction of natural organic matter with acid mine drainage: authigenic mineralization (case study of Ursk sulfide tailings, Kemerovo Region, Russia). J Geochem Explor 211:106456. https://doi.org/10.1016/j.gexplo.2019.106456

Myagkaya IN, Saryg-ool BYu, Surkov ON, Zhmodik SM, Lazareva EV, Taran OP (2021) Natural organic matter from the dispersion train of gold sulfide tailings: group composition and fractionation of elements: case study of Ursk Tailings, Kemerovo Region, Siberia. Geochem Explor Environ Anal 21(1):geochem2020-052. https://doi.org/10.1144/geochem2020-052

Naidu G, Ryu S, Thiruvenkatachari R, Choi Y, Jeong S, Vigneswaran S (2019) A critical review on remediation, reuse, and resource recovery from acid mine drainage. Environ Pollut 247:1110–1124. https://doi.org/10.1016/j.envpol.2019.01.085

Najamuddin N, Prartono T, Sanusi HS, Nurjaya IW (2016) Seasonal distribution and geochemical fractionation of heavy metals from surface sediment in a tropical estuary of Jeneberang River, Indonesia. Mar Pollut Bull 111:456–462. https://doi.org/10.1016/j.marpolbul.2016.06.106

Navarro A, Cardellach E, Corbella M (2009) Mercury mobility in mine waste from Hg-mining areas in Almería, Andalusia (Se Spain). J Geochem Explor 101(3):236–246. https://doi.org/10.1016/j.gexplo.2008.08.004

Nieva NE, Borgnino L, García MG (2018) Long term metal release and acid generation in abandoned mine wastes containing metal-sulphides. Environ Pollut 242:264–276. https://doi.org/10.1016/j.envpol.2018.06.067

Paquette KE, Helz GR (1997) Inorganic speciation of mercury in sulfidic waters: the importance of zero-valent sulfur. Environ Sci Technol 31(7):2148–2153. https://doi.org/10.1021/es961001n

Pestana MHD, Lechler P, Formoso MLL, Miller J (2000) Mercury in sediments from gold and copper exploitation areas in the Camaqua River Basin, southern Brazil. J S Am Earth Sci 13(6):537–547. https://doi.org/10.1016/S0895-9811(00)00039-0

Petrosyan VS (1999) Mercury pollution: causes and consequences. Ekol Promysh Ross, pp 34–38 (**in Russian**)

Petrov LL, Kornakov YN, Persikova LA, Anchutina EA (1999) Reference samples of Lake Baikal bottom sediments—an essential part of regional collection of reference samples. Int J Environ Anal Chem 74(1–4):275–288

Pokrovsky OS, Schott J (2002) Iron colloids/organic matter associated transport of major and trace elements in small boreal rivers and their estuaries (NW Russia). Chem Geol 190(1–4):141–179. https://doi.org/10.1016/S0009-2541(02)00115-8

Qian J, Skyllberg U, Frech W, Bleam WF, Bloom PR, Petit PE (2002) Bonding of methyl mercury to reduced sulfur groups in soil and stream organic matter as determined by x-ray absorption spectroscopy and binding affinity studies. Geochim Cosmochim Acta 66(22):3873–3885. https://doi.org/10.1016/S0016-7037(02)00974-2

Qiu G, Feng X, Meng B, Sommar J, Gu C (2012) Environmental geochemistry of an active Hg mine in Xunyang, Shaanxi Province, China. Appl Geochem 27(12):2280–2288. https://doi.org/10.1016/j.apgeochem.2012.08.003

Qiu G, Feng X, Meng B, Zhang C, Gu C, Du B, Lin Y (2013) Environmental geochemistry of an abandoned mercury mine in Yanwuping, Guizhou Province, China. Environ Res 125:124–130. https://doi.org/10.1016/j.envres.2013.01.008

Ravichandran M (2004) Interactions between mercury and dissolved organic matter—a review. Chemosphere 55(3):319–331. https://doi.org/10.1016/j.chemosphere.2003.11.011

Rimondi V, Gray JE, Costagliola P, Vaselli O, Lattanzi P (2012) Concentration, distribution, and translocation of mercury and methylmercury in mine-waste, sediment, soil, water, and fish collected near the Abbadia San Salvatore mercury mine, Monte Amiata district, Italy. Sci Total Environ 414:318–327. https://doi.org/10.1016/j.scitotenv.2011.10.065

Roberts S, Adams JK, Mackay AW, Swann GE, McGowan S, Rose NL, Panizzo V, Yang H, Vologina E, Sturm M, Shchetnikov AA (2020) Mercury loading within the Selenga River basin and Lake Baikal, Siberia. Environ Pollut 259:113814. https://doi.org/10.1016/j.envpol.2019.113814

Rytuba JJ (2000) Mercury mine drainage and processes that control its environmental impact. Sci Total Environ 260(1–3):57–71. https://doi.org/10.1016/S0048-9697(00)00541-6

Sarkar D, Essington ME, Misra KC (1999) Adsorption of mercury (II) by variable charge surfaces of quartz and gibbsite. Soil Sci Soc Am J 63(6):1626–1636. https://doi.org/10.2136/sssaj1999.6361626x

Saryg-ool BYu, Myagkaya IN, Kirichenko IS, Gustaytis MA, Shuvaeva OV, Zhmodik SM, Lazareva EV (2017) Redistribution of elements between wastes and organic-bearing material in the dispersion train of gold-bearing sulfide tailings: part i. Geochemistry and mineralogy. Sci Tot Environ 581:460–471. https://doi.org/10.1016/j.scitotenv.2016.12.154

Saryg-ool BYu, Myagkaya IN, Kirichenko IS, Gustaytis MA, Shuvaeva OV, Zhmodik SM, Lazareva EV (2020) Redistribution and speciation of elements in gold-bearing sulfide mine tailings interbedded with natural organic matter: case study of Novo-Ursk deposit, Kemerovo Region, Siberia. Geochem-Explor Env Anal 20(3):323–336. https://doi.org/10.1144/geochem2019-043

Savenko VS (2006) Chemical composition of suspended matter in world rivers. GEOS, Moscow (**in Russian**)

Savichev OG (2003) Rivers of the Tomsk region: condition, use and protection. TPU Publishing House, Tomsk (**in Russian**)

Schaider LA, Senn DB, Estes ER, Brabander DJ, Shine JP (2014) Sources and fates of heavy metals in a mining-impacted stream: temporal variability and the role of iron oxides. Sci Tot Environ 490:456–466. https://doi.org/10.1016/j.scitotenv.2014.04.126

Scherbov BL, Lazareva EV (2010) Migration factors of radionuclides and heavy metals during forest fires in Siberia. Adv Environ Res 4:99–120

Schmid T, Rico C, Rodríguez-Rastrero M, Sierra MJ, Díaz-Puente FJ, Pelayo M, Millán R (2013) Monitoring of the mercury mining site Almadén implementing remote sensing technologies. Environ Res 125:92–102. https://doi.org/10.1016/j.envres.2012.12.014

Schuster E (1991) The behavior of mercury in the soil with special emphasis on complexation and adsorption processes-a review of the literature. Water Air Soil Poll 56(1):667–680

Seal RR, Hammarstrom JM (2003) Geoenvironmental models of mineral deposits: examples from massive sulfide and gold deposits.

In: Blowes JL, Ritchie DW (eds) Environmental Aspects of Mine Wastes, vol 31. Mineralogical Assoc of Canada, pp 11–50
Shevyrev LT (2013) Patterns of volatiles on the Earth's surface: possible historic and metallogenic interpretation. Mercury. Bull Voronezh State Univ Ser Geol 2:106–117 (**in Russian**)
Shulkin VM, Ivlev DI (2013) Mercury contents in natural waters of the Primoriye region. Bull DVO RAN 2:98–105 (**in Russian**)
Skyllberg ULF, Qian JIN, Frech W, Xia K, Bleam WF (2003) Distribution of mercury, methyl mercury and organic sulphur species in soil, soil solution and stream of a boreal forest catchment. Biogeochemistry 64(1):53–76
State Standard (2004) Working Document GOST 8.135–2004 State system for ensuring the uniformity of measurements. In: Weight amounts of standard materials for buffer solutions: operational pH standards of 2nd and 3rd classes, Technical and metrological characteristics and methods of their determination.
Stevenson FJ (1994) Humus chemistry: genesis composition, reactions. Wiley
Sundaray SK, Nayak BB, Lin S, Bhatta D (2011) Geochemical speciation and risk assessment of heavy metals in the river estuarine sediments – a case study: Mahanadi basin. India J Hazard Mater 186(2–3):1837–1846. https://doi.org/10.1016/j.jhazmat.2010.12.081
Telmer K, Costa M, Angélica RS, Araujo ES, Maurice Y (2006) The source and fate of sediment and mercury in the Tapajós River, Pará, Brazilian Amazon: ground-and space-based evidence. J Environ Manag 81(2):101–113. https://doi.org/10.1016/j.jenvman.2005.09.027
Tokarev VN, Shatilova GA, Kotik OP (2004) Geological map of the Russian Federation. Scale 1:200000, 2nd edit, Series Kuzbass, Sheet N-45-XIV, Explanatory Note, St. Petersburg (**in Russian**)
Tromans D, Meech JA, Veiga MM (1996) Natural organics and environmental stability of mercury: Electrochemical considerations. J Electrochem Soc 143(6):L123
Tseng CM, Amouroux D, Abril G, Tessier E, Etcheber H, Donard OFX (2001) Speciation of mercury in a fluid mud profile of a highly turbid macrotidal estuary (Gironde, France). Environ Sci Technol 35(13):2627–2633. https://doi.org/10.1021/es001750b
Ullrich SM, Tanton TW, Abdrashitova SA (2001) Mercury in the aquatic environment: a review of factors affecting methylation. Crit Rev Environ Sci Technol 31(3):241–293. https://doi.org/10.1080/20016491089226
Ullrich SM, Ilyushchenko MA, Uskov GA, Tanton TW (2007) Mercury distribution and transport in a contaminated river system in Kazakhstan and associated impacts on aquatic biota. Appl Geochem 22(12):2706–2734. https://doi.org/10.1016/j.apgeochem.2007.07.005
Umezaki Y, Iwamoto K (1971) The determination of submicrogram amounts of mercury. Jpn Analyst 20:173–179
Vonk JE, Tank SE, Bowden WB, Laurion I, Vincent WF, Alekseychik P, Wickland KP (2015) Reviews and syntheses: effects of permafrost thaw on Arctic aquatic ecosystems. Biogeosciences 12(23):7129–7167. https://doi.org/10.5194/bg-12-7129-2015
Walcarius A, Devoy J, Bessiere J (1999) Electrochemical recognition of selective mercury adsorption on minerals. Environ Sci Technol 33(23):4278–4284. https://doi.org/10.1021/es990525v
Wallschläger D, Desai MV, Spengler M, Wilken RD (1998a) Mercury speciation in floodplain soils and sediments along a contaminated river transect. J Environ Qual 27(5):1034–1044. https://doi.org/10.2134/jeq1998.00472425002700050008x
Wallschläger D, Desai MV, Spengler M, Windmöller CC, Wilken RD (1998b) How humic substances dominate mercury geochemistry in contaminated floodplain soils and sediments. J Environ Qual 27(5):1044–1054. https://doi.org/10.2134/jeq1998.00472425002700050009x
Wang W, Wen B, Zhang S, Shan XQ (2003) Distribution of heavy metals in water and soil solutions based on colloid-size fractionation. Int J Environ Anal Chem 83(5):357–365. https://doi.org/10.1080/0306731031000104704
Water Quality (2000) Environmental Health Criteria for Surface Water. Working Document 2.1.5.980–00. Ministry of Health of the Russian Federation, Moscow (**in Russian**)
Water Quality (2007) Environmental Health Criteria. Maximum Permissible Limits of Chemical Elements in Drinking and Household Water. Working Document GN 2.1.5.2280–07, Moscow (**in Russian**)
Willis CE, Louis VLS, Kirk JL, Pierre KAS, Dodge C (2019) Tailings ponds of the Athabasca oil sands region, Alberta, Canada, are likely not significant sources of total mercury and methylmercury to nearby ground and surface waters. Sci Tot Environ 647:1604–1610. https://doi.org/10.1016/j.scitotenv.2018.08.083
World Health Organization (1990) International program on chemical safety, environmental health criteria 101. Methylmercury, Geneva, p 148
World Health Organization (2017) Guidelines for drinking water quality, 4th Edit, with 1st Addendum. WHO, Geneva
Xia K, Skyllberg UL, Bleam WF, Bloom PR, Nater EA, Helmke PA (1999) X-ray absorption spectroscopic evidence for the complexation of Hg (II) by reduced sulfur in soil humic substances. Environ Sci Technol 33(2):257–261. https://doi.org/10.1021/es980433q
Xu G, Li P, Lu K, Tantai Z, Zhang J, Ren Z, Cheng Y (2019) Seasonal changes in water quality and its main influencing factors in the Dan River basin. CATENA 173:131–140. https://doi.org/10.1016/j.catena.2018.10.014
Zhang L, Jin Y, Lu J, Zhang C (2009) Concentration, distribution and bioaccumulation of mercury in the Xunyang mercury mining area, Shaanxi Province. China Appl Geochem 24(5):950–956. https://doi.org/10.1016/j.apgeochem.2009.02.027